ALEX(01)-TR-77-12

LEVEL II

RELATIONSHIPS BETWEEN NOISE AND mb BIAS APPLIED TO SEISMIC STATION SITE SELECTION AND PERFORMANCE EVALUATION

12

TECHNICAL REPORT NO. 12

VELA NETWORK EVALUATION AND AUTOMATIC PROCRESSING RESEARCH

Prepared by
Donald L. Dietz and Robert L. Sax

TEXAS INSTRUMENTS INCORPORATED
Equipment Group
Post Office Box 6015
Dallas, Texas 75222

Prepared for

AIR FORCE TECHNICAL APPLICATIONS CENTER
Alexandria, Virginia 22314

Sponsored by

ADVANCED RESEARCH PROJECTS AGENCY
Nuclear Monitoring Research Office
ARPA Program Code No. 7F10
ARPA Order No. 2551

23 March 1978

Acknowledgment: This research was supported by the Advanced Research Projects Agency, Nuclear Monitoring Research Office, under Project VELA-UNIFORM, and accomplished under the technical direction of the Air Force Technical Applications Center under Contract Number F08606-77-C-0004.

ALEX(01)-TR-77-12

RELATIONSHIPS BETWEEN NOISE AND mb BIAS APPLIED TO SEISMIC STATION SITE SELECTION AND PERFORMANCE EVALUATION

TECHNICAL REPORT NO. 12

VELA NETWORK EVALUATION AND AUTOMATIC PROCRESSING RESEARCH

Prepared by
Donald L. Dietz and Robert L. Sax

TEXAS INSTRUMENTS INCORPORATED
Equipment Group
Post Office Box 6015
Dallas, Texas 75222

Prepared for

AIR FORCE TECHNICAL APPLICATIONS CENTER
Alexandria, Virginia 22314

Sponsored by

ADVANCED RESEARCH PROJECTS AGENCY
Nuclear Monitoring Research Office
ARPA Program Code No. 7F10
ARPA Order No. 2551

23 March 1978

Acknowledgment: This research was supported by the Advanced Research Projects Agency, Nuclear Monitoring Research Office, under Project VELA-UNIFORM, and accomplished under the technical direction of the Air Force Technical Applications Center under Contract Number F08606-77-C-0004.

UNCLASSIFIED

SECURITY CLASSIFICATION OF THIS PAGE (When Data Entered)

REPORT DOCUMENTATION PAGE	READ INSTRUCTIONS BEFORE COMPLETING FORM
1. REPORT NUMBER	2. GOVT ACCESSION NO. 3. RECIPIENT'S CATALOG NUMBER
4. TITLE (and Subtitle) (6) RELATIONSHIPS BETWEEN NOISE AND m_b BIAS APPLIED TO SEISMIC STATION SITE SELECTION AND PERFORMANCE EVALUATION,	5. TYPE OF REPORT & PERIOD COVERED: Technical
(14) TI-ALEX(01)-TR-77-12	6. PERFORMING ORG. REPORT NUMBER
7. AUTHOR(s) (10) Donald L. Dietz and Robert L. Sax	8. CONTRACT OR GRANT NUMBER(s): F08606-77-C-0004
9. PERFORMING ORGANIZATION NAME AND ADDRESS: Texas Instruments Incorporated, Equipment Group, Dallas, Texas 75222	10. PROGRAM ELEMENT, PROJECT, TASK AREA & WORK UNIT NUMBERS: VELA T/7705/B/ETR
11. CONTROLLING OFFICE NAME AND ADDRESS: Advanced Research Projects Agency, 1400 Wilson Boulevard, Arlington, Virginia 22209	(11) 12. REPORT DATE: 23 March 1978 13. NUMBER OF PAGES: 103
14. MONITORING AGENCY NAME & ADDRESS (if different from Controlling Office): Air Force Technical Applications Center, VELA Seismological Center, Alexandria, Virginia 22314	15. SECURITY CLASS. (of this report): UNCLASSIFIED 15a. DECLASSIFICATION/DOWNGRADING SCHEDULE

16. DISTRIBUTION STATEMENT (of this Report)

(9) Technical rept. 2

APPROVED FOR PUBLIC RELEASE, DISTRIBUTION UNLIMITED

(12) 105 p.

17. DISTRIBUTION STATEMENT (of the abstract entered in Block 20, if different from Report)

18. SUPPLEMENTARY NOTES

(15) F08606-77-C-0004, ARPA Order-2551

ARPA Order No. 2551

19. KEY WORDS (Continue on reverse side if necessary and identify by block number)

Empirical m_b bias - noise relationship
Network m_b bias
Seismic noise
Station site selection
Noise zones
Seasonal noise
Network capability
Tectonics

20. ABSTRACT (Continue on reverse side if necessary and identify by block number)

An analysis of forty-six stations with known m_b bias, noise amplitude, and tectonic structure showed that a relationship exists between these three parameters. A wide range of slopes in the relationship of noise magnitude and bias were examined. A slope of one applied to several normal groupings of noise levels provided a precise means of predicting the performance of seismic stations within large geographical areas. This interpretation resulted in three distinct noise zones within interior continental areas, and

DD FORM 1 JAN 73 1473 EDITION OF 1 NOV 65 IS OBSOLETE

UNCLASSIFIED

SECURITY CLASSIFICATION OF THIS PAGE (When Data Entered)

405 076

20. continued

very high coastal noise zones in other areas. For the case of zero m_b bias, low noise zones have 1.62 mμ zero-to-peak noise; medium, 3.79 mμ ; high, 9.10 mμ ; and very high (coastal) zones, 15.80 mμ . The standard deviation of these zones is approximately 0.08 magnitude units. The zones are believed to extend over large geographical areas of the earth, but are not as closely correlated with tectonic province as magnitude bias. This model and others for describing relationships between noise levels and bias were statistically tested with positive results at the 95% and 99% level of confidence. The results of the models and measurements of noise and bias were used to evaluate hypothetical 100 station networks in terms of detection and location capability and bias of network magnitude determinations.

We believe that our interpretation of geographical noise zones can be a useful tool in selecting the sites of seismic stations and predicting their performance. Associated geophysical and geological factors should be investigated to more fully understand the physical mechanism of noise zoning and to improve site selection given the sparse amount of available information on actual measurements of bias and noise. It would also seem advisable to greatly extend the data base upon which our conclusions were based.

ABSTRACT

An analysis of forty-six stations with known m_b bias, noise amplitude, and tectonic structure showed that a relationship exists between these three parameters. A wide range of slopes in the relationship of noise magnitude and bias were examined. A slope of one applied to several normal groupings of noise levels provided a precise means of predicting the performance of seismic stations within large geographical areas. This interpretation resulted in three distinct noise zones within interior continental areas, and very high coastal noise zones in other areas. For the case of zero m_b bias, low noise zones have 1.62 $m\mu$ zero-to-peak noise; medium, 3.79 $m\mu$; high, 9.10 $m\mu$; and very high (coastal) zones, 15.80 $m\mu$. The standard deviation of these zones is approximately 0.08 magnitude units. The zones are believed to extend over large geographical areas of the earth, but are not as closely correlated with tectonic province as magnitude bias. This model and others for describing relationships between noise levels and bias were statistically tested with positive results at the 95% or 99% level of confidence. The results of the models and measurements of noise and bias were used to evaluate hypothetical 100 station networks in terms of detection and location capability and bias of network magnitude determinations.

We believe that our interpretation of geographical noise zones can be a useful tool in selecting the sites of seismic stations and predicting their performance. Associated geophysical and geological factors should be investigated to more fully understand the physical mechanism of noise zoning and to improve site selection given the sparse amount of available information on actual measurements of bias and noise. It would also seem advisable to greatly extend the data base upon which our conclusions were based.

ACKNOWLEDGMENT

The authors gratefully acknowledge Nolan S. Snell for his help in modifying the program NETPROB, and Alan C. Strauss for his many helpful suggestions on writing this report.

TABLE OF CONTENTS

LIST OF FIGURES

LIST OF FIGURES
(continued)

LIST OF FIGURES
(continued)

LIST OF TABLES

SUMMARY

We carried out this investigation to improve our estimates of the detection capability of seismic stations and seismic networks. The scope of the investigation is to improve the estimates of detection capability by utilizing seismic noise and signal bias measurements at existing stations and by improving our ability to predict the performance at sites where signal and noise measurements are not yet available.

We statistically analyzed published data from forty-six seismic observatories distributed around the world. The data consisted of measurements of short-period seismic noise and measurements of average bias of m_b determinations. Also included was the tectonic classification of the regions where the stations are located. In order to interpret seasonal variations of the noise and the influence of coastline proximity, world maps of monthly averages of seismic noise were also included.

The approach of our investigation was to propose and statistically test a number of hypothetical empirical relationships between noise levels at seismic stations and the bias of m_b determinations. One of our purposes was to improve our determinations of the detection capability by taking into account the bias of signal magnitude measurements as well as the observed noise levels at the site.

An even more important goal of our investigation was to be able to accurately predict noise levels and m_b bias at the sites of possible future seismic stations. Our approach was to examine noise and bias data for factors which most accurately predict m_b bias and noise. Given such a basis, we would then sub-divide the Earth's continental crust into large

regional zones. The complex pattern of noise levels in each zone, if corrected for bias, would be characterized everywhere within the zone by a single noise level of equivalent-zero-bias noise plus small normal random errors. Equivalent-zero-bias noise is the noise level that would be predicted by a given noise-bias relationship for a zero-bias station. For example, there would be low-noise zones, medium-noise zones, high-noise zones, and very high coastal-noise zones. It would be a much more promising task to define the boundaries of several such zones using sparse data from existing seismic stations than to arbitrarily contour the world for both seismic noise levels and magnitude bias. The utility of our approach will depend on the accuracy and precision with which our empirical models predict the performance of seismic stations. This utility is of course limited by other important factors beyond the scope of this investigation. These are local geology, local sources of propagating noise, environmental effects, and engineering considerations.

The empirical results of our investigation indicated strong statistical significance in a straight-line correlative relationship between m_b bias and noise magnitude. We carried out an exhaustive search to find the slope of the straight-line relationship between noise magnitude and m_b bias. In doing this, we discovered that a slope of one, applied to four distinctly separated populations, resulted in a minimum variance solution. The variance of the four selected groups was low enough for us to use measurements of m_b bias and noise magnitude to unambiguously classify stations by their low, medium, high, or very high coastal equivalent-zero-bias noise levels. Furthermore, such classifications were usually observed to be consistent over large regions of the continental crust.

The slope of one relationship between m_b bias and noise magnitude greatly simplified the analysis of the combined effect of noise and bias on station detection capability. The slope of one relationship implies that all stations in a particular noise group, such as the low-noise group are, except

for normal variability, equally effective as detectors of seismic events. This occurs because neither bias nor noise are dominant factors in this representation. The advantage of having low noise is exactly canceled by the disadvantage of having low (negative) bias. For example, if a station in a noise group is found to have a noise level 0.2 magnitude units lower than a zero-bias seismic station, then it can be expected to have a magnitude bias exactly 0.2 units lower, which in this case would be -0.2 magnitude bias. Consequently, the detectability of events is unchanged. This same implication, of course, applies to all of the noise groups.

As previously pointed out, classifying noise into discrete groups is only useful because the populations are separated well enough for us to unambiguously use measurements to classify the stations, and to map boundaries of each noise group consistently over large areas of the Earth. The combined standard deviation of noise from all four noise groups was found to be 0.08 as compared to a standard deviation of 0.44 from a single noise mean for all of the data. As shown in Figure S-1, the distance between adjacent populations means were observed to be between 0.24 and 0.37 magnitude units. A measure of the detectability of these groups can be obtained from these figures by dividing the difference between the adjacent population means by the standard deviation of the populations. This indicates detectabilities greater than three and thus a very high probability of correctly determining the equivalent-zero-bias noise group from measurements of noise level and bias.

We are of the opinion that the consistency of zoning of equivalent-zero-bias noise means over large areas of the earth is reasonably shown in Figure S-2. For example, the central Canadian Shield and large areas of the western United States are low-noise areas. Southern Africa and southern Australia appear to be high-noise areas. We are encouraged to believe that with considerably more data, we might possibly achieve our goal of simplifying and optimizing seismic site selection, in this way. Note that the map in

NOISE GROUPS FOR 33 STATIONS WITH OBSERVED NOISE

Noise Group	Noise Magnitude $\log_{10}$(p-p ampl.)	Noise Amplitude (0-p, mμ)	Standard Deviation of Noise Magnitude
Low	0.51	1.62	0.11
Medium	0.88	3.79	0.08
High	1.26	9.10	0.04
Coastal (very high)	1.50	15.80	0.08

SD of noise for entire model = 0.08

FIGURE S-1

MEANS AND STANDARD DEVIATIONS OF
EQUIVALENT-ZERO-BIAS NOISE GROUPS

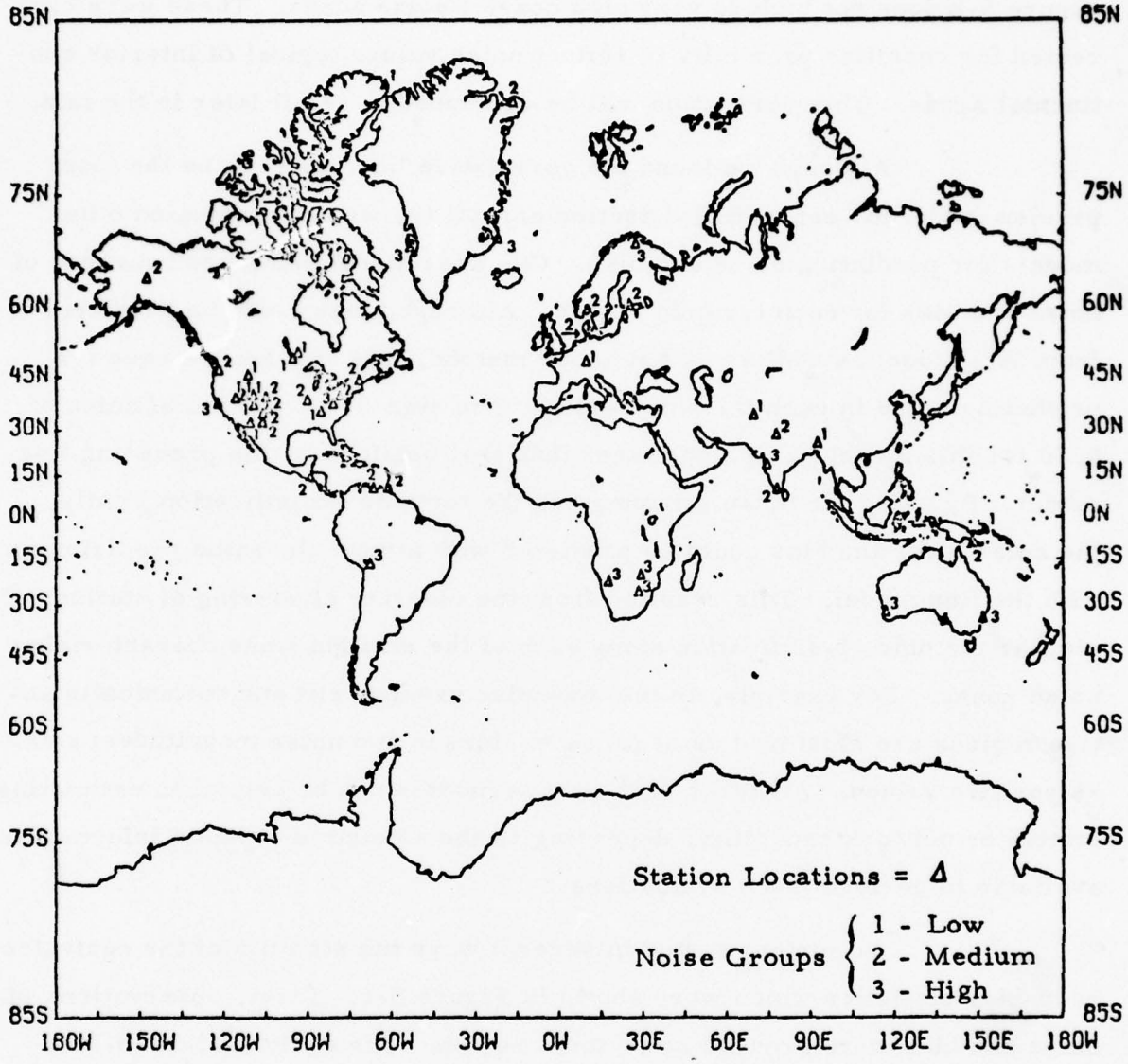

FIGURE S-2

GEOGRAPHIC DISTRIBUTION OF NOISE GROUPS FOR 46 STATIONS WITH NOISE CORRECTED FOR COASTLINE PROXIMITY

Figure S-2 does not include very high coastal-noise zones. These were corrected for coastline proximity to reflect noise values typical of interior continental areas. This correction will be described in detail later in the text.

Although we found the correlative line model to be the most precise model for estimating detection capability, we also evaluated other models for predicting noise and bias. One such model computed averages of noise and bias for each tectonic region. Although, bias could be predicted from this model as well as by any other method, this was not the case for predicting noise in each tectonic region. The standard deviation of noise of 0.30 for this model was much larger than that obtained by the preceding line model. By using the noise grouping and the tectonic classification jointly, the noise level and bias could be predicted with almost the same precision as with the line model. This resulted from the discrete clustering of stations of similar tectonic classification along each of the straight lines characterizing noise zones. For example, in the low-noise groups, rift and tectonically active regions are clustered as negative m_b biases and noise magnitudes; shields, as positive values. All three of the above models can be helpful in estimating station or network capability, depending on the amount of a priori information available to perform such evaluations.

We further tested in several ways the stability of the equivalent-zero-bias statistics which were shown in Figure S-1. First, observations of noise and bias were grouped by tectonic region. The equivalent-zero-bias noise means and standard deviations were computed for each joint classification of noise group and tectonic type. The results, shown in Figure S-3, show excellent stability as seen by comparison of the noise means, $\overline{N}_{jk}$, shown for each tectonic group. Second, the equivalent-zero-bias noise means shown in Figure S-1, were re-computed using 13 additional stations not used in the initial estimates, because the noise figures were less well defined and possibly of lesser quality. Again, only small changes occurred in the resultant

Definition of indices indicating type of noise groups and tectonic types

j =	1	Low noise	
	2	Medium	
	3	High	
	4	Very high (coastal)	
	5	All above groups combined	

k =	1	Rift	
	2	Platform or fold belt	
	3	Shield	
	4	All above groups combined	

A. 33 Joint Classifications of Stations by Noise Zone and Tectonic Region

k \ j	1	2	3	4	5
1	5	2	0	0	7
2	3	3	5	0	11
3	2	1	5	7	15
4	10	6	10	7	33

Table entries represent the number of stations in each joint classification.

B. Noise Prediction by Line Model Applied to Stations in Different Tectonic Regions

N_{jk}: Average noise magnitude $\log_{10}$(p-p) B_{jk}: Average P-wave magnitude bias

$\overline{N}_{jk} = N_{jk} - B_{jk} + \text{Error}$ (error considered normal)

$\overline{N}_{jk}$:

k \ j	1	2	3	4
1	0.51	0.89	-	-
2	0.50	0.91	1.28	-
3	0.52	0.78	1.24	1.50
4	0.51	0.88	1.26	1.50

j	1	2	3	4	5
B_{j4}	0.11	0.08	0.04	0.08	0.08
N_{j4}	0.11	0.08	0.04	0.08	0.08
df	9	5	9	6	29

df - degrees of freedom

FIGURE S-3

STATISTICS OF THE SLOPE OF ONE STRAIGHT LINE RELATIONSHIP BETWEEN NOISE MAGNITUDE AND BIAS RELATED TO JOINT CLASSIFICATION BY NOISE ZONE AND REGIONAL TECTONICS

$$Y(f,x) = Y_o(f)\left[\frac{x}{x_o}\right]^{k(f)}$$

where

$$\ln Y_o(f) = \left[\alpha e^{-\beta(\ln(f/\gamma))^2}\right] - \ln 50$$

$$k(f) = a e^{-b(\ln(f/c))^2}$$

constants:

x_o	α	β	γ	a	b	c	f
350 km	7.61	0.382	0.20	-0.878	0.169	1.40	0.25 Hz

α, β, γ, a, b, c	empirical constants
f	frequency (Hz)
x_o	distance of a master station from the coastline
x	distance from the nearest coastline
Y_o	average noise amplitude mμ (p-p) at master station
Y	noise amplitude mμ (p-p) at some reference point, x.

FIGURE S-4

BASIS OF NOISE CORRECTION FOR COASTLINE PROXIMITY
GRIFFIN (1963)

equivalent-zero-bias noise group mean values. Third, since we are primarily interested in network performance for stations not located at very high coastal-noise zones, those stations were corrected for the noise expected due to coastline proximity, by using a method based on the equations shown in Figure S-4. Figure S-5 shows the histogram of the noise groups before correcting for coastline proximity, and Figure S-6 the groups after correcting for coastline proximity. It can be seen that very little change occurred in the population means, and that there are now only three noise groups (low-, medium-, and high-noise) remaining.

An important consideration in evaluating networks is the location of high-noise coastal zones with strong seasonal variations related to noise propagating from the ocean. The location of the coastal zones are roughly indicated by continental areas not jointly enclosed by the peak-to-peak 50 mμ contours representing seasonal extremes shown in Figure S-7. Those broad continental areas of very high coastal-noise, such as the east coast of North America which extends well into the continent, appear to be related to extensive continental shelf areas where there are thick wedges of recent marine sediments. The existance of such sediments may play an important role in enhancing propagating ocean noise far from the actual coastline during noisy seasons. Also of interest is an area apparently equivalent to a seasonally stable continental region which includes northern Australia and islands well north of Australia. This oceanic region north of Australia thus appears to be free of large seasonal variations, and does not appear to behave like a very high coastal-noise zone.

Our results were applied to estimating the detection and location capability of a hypothetical large network of 72 single stations and 28 arrays located in the southern hemisphere and circum-Pacific to reach into areas sparsely covered by seismic stations. We show in Figure S-8 that in addition to the locations of WWSSN (World-Wide Standard Seismograph

A. 33 STATIONS WITH OBSERVED NOISE

STATION VALUES

m = 1.00

I	Name	Bias	Noise	$\overline{N}$
1	EUR	-0.240	0.400	0.640
2	BKUT	-0.180	0.430	0.610
3	UBO	-0.110	0.176	0.286
4	BOZ	-0.060	0.398	0.458
5	DUG	-0.150	0.398	0.548
6	CPO	-0.070	0.398	0.468
7	KBI	0.090	0.562	0.472
8	SHL	0.110	0.683	0.573
9	EBRT	0.120	0.716	0.596
10	RKON	0.280	0.716	0.436
11	ALQ	-0.200	0.710	0.910
12	LCNM	-0.170	0.700	0.870
13	COL	0.010	0.990	0.980
14	BFPA	0.060	1.000	0.940
15	PTSM	0.090	0.900	0.810
16	MDI	0.330	1.109	0.779
17	LSNM	0.0	1.300	1.300
18	LPS	0.340	1.363	1.323
19	PMG	0.100	1.366	1.266
20	LPB	0.070	1.253	1.183
21	BLWV	0.120	1.450	1.330
22	NOE	-0.140	1.102	1.242
23	KON	0.070	1.318	1.248
24	KOD	0.060	1.329	1.269
25	BTL	-0.070	1.134	1.204
26	MUP	0.190	1.443	1.253
27	WIM	-0.090	1.331	1.421
28	PRE	-0.070	1.331	1.401
29	GDH	0.0	1.575	1.575
30	KEV	0.020	1.559	1.539
31	HHW	0.150	1.637	1.487
32	POO	0.170	1.643	1.473
33	KTG	0.020	1.628	1.608

Noise Groups		Stations
	1 Low	1-10
	2 Medium	11-16
	3 High	17-26
	4 Very High (Coastal).	27-33

HISTOGRAM OF $\overline{N}$

Bin Index	Center $\overline{N}$ of Bin	# in Bin	
1	-0.50	0	
2	-0.45	0	
3	-0.40	0	
4	-0.35	0	
5	-0.30	0	
6	-0.25	0	
7	-0.20	0	
8	-0.15	0	
9	-0.10	0	
10	-0.05	0	
11	0.00	0	
12	0.05	0	
13	0.10	0	
14	0.15	0	
15	0.20	1	X
16	0.25	1	X
17	0.30	1	X
18	0.35	2	XX
19	0.40	4	XXXX
20	0.45	5	XXXXX
21	0.50	7	XXXXXXX ←
22	0.55	8	XXXXXXXX
23	0.60	5	XXXXX
24	0.65	4	XXXX
25	0.70	3	XXX
26	0.75	2	XX
27	0.80	3	XXX
28	0.85	5	XXXXX ←
29	0.90	5	XXXXX
30	0.95	4	XXXX
31	1.00	3	XXX
32	1.05	1	X
33	1.10	1	X
34	1.15	4	XXXX
35	1.20	7	XXXXXXX
36	1.25	10	XXXXXXXXXX ←
37	1.30	9	XXXXXXXXX
38	1.35	8	XXXXXXXX
39	1.40	7	XXXXXXX
40	1.45	5	XXXXX
41	1.50	6	XXXXXX ←
42	1.55	5	XXXXX
43	1.60	3	XXX
44	1.65	2	XX
45	1.70	1	X
46	1.75	0	
47	1.80	0	
48	1.85	0	
49	1.90	0	
50	1.95	0	

STATION GROUPING

Bin Index										
1										
2										
3										
4										
5										
6										
7										
8										
9										
10										
11										
12										
13										
14										
15	3									
16	3									
17	3									
18	3	10								
19	4	6	7	10						
20	4	5	6	7	10					
21	4	5	6	7	8	9	10			
22	1	2	5	6	7	8	9			
23	1	2	5	8	9					
24	1	2	8	9						
25	1	2	16							
26	15	16								
27	12	15	16							
28	11	12	14	15	16					
29	11	12	13	14	15					
30	11	12	13	14						
31	11	13	14							
32	13									
33	20									
34	20	22	23	25						
35	19	20	22	23	24	25	26			
36	17	18	19	20	21	22	23	24	25	26
37	17	18	19	21	22	23	24	25	26	
38	17	18	19	21	26	26	27	28		
39	17	18	21	27	28	31	32			
40	27	28	30	31	32					
41	27	28	29	30	31	32				
42	29	30	31	32	33					
43	29	30	33							
44	29	33								
45	33									
46										
47										
48										
49										
50										

FIGURE S-5

HISTOGRAMS OF STATION NOISE LEVELS BY $\overline{N}$, BIN SIZE = 0.200;
75% OVERLAP, $\overline{N} = N - mB$, WHERE m = 1.00

B. 33 STATIONS WITH NOISE CORRECTED FOR OCEAN NOISE

STATION VALUES

m = 1.00

I	Name	Bias	Noise	$\overline{N}$
1	EDB	-0.240	0.400	0.640
2	RKUT	-0.180	0.430	0.610
3	UBO	-0.110	0.176	0.286
4	BOZ	-0.060	0.398	0.458
5	DUG	-0.150	0.398	0.548
6	CPO	-0.070	0.398	0.468
7	KRL	0.090	0.563	0.472
8	SHL	0.110	0.523	0.413
9	EBMT	0.120	0.716	0.596
10	RKON	0.280	0.716	0.436
11	ALQ	-0.200	0.710	0.910
12	LCNM	-0.170	0.700	0.870
13	COL	0.010	0.938	0.928
14	BPPA	0.060	1.000	0.940
15	BTNM	0.090	0.900	0.810
16	LSNM	0.0	1.021	1.021
17	LPS	0.040	0.991	0.951
18	PMG	0.100	0.994	0.894
19	WDI	0.330	1.109	0.779
20	KON	0.070	0.946	0.876
21	KOD	0.060	0.957	0.897
22	MNR	0.190	1.071	0.881
23	NOR	-0.140	0.730	0.870
24	LPB	0.070	1.203	1.133
25	BLWV	0.120	1.450	1.330
26	BUL	-0.070	1.134	1.204
27	WIN	-0.090	1.119	1.209
28	PRE	-0.070	1.279	1.349
29	GDH	0.0	1.203	1.203
30	KEV	0.020	1.187	1.167
31	MUN	0.150	1.265	1.115
32	POO	0.170	1.271	1.101
33	KTG	0.020	1.256	1.236

Noise-Groups		Stations
	1 Low	1-10
	2 Medium	11-23
	3 High	24-33

HISTOGRAM OF $\overline{N}$

Bin Index	Center $\overline{N}$ of Bin	# in Bin	
1	-0.50	0	
2	-0.45	0	
3	-0.40	0	
4	-0.35	0	
5	-0.30	0	
6	-0.25	0	
7	-0.20	0	
8	-0.15	0	
9	-0.10	0	
10	-0.05	0	
11	0.00	0	
12	0.05	0	
13	0.10	0	
14	0.15	0	
15	0.20	1	X
16	0.25	1	X
17	0.30	1	X
18	0.35	3	XXX
19	0.40	5	XXXXX
20	0.45	6	XXXXXX
21	0.50	7	XXXXXXX ←
22	0.55	7	XXXXXXX
23	0.60	4	XXXX
24	0.65	3	XXX
25	0.70	3	XXX
26	0.75	2	XX
27	0.80	8	XXXXXXXX
28	0.85	11	XXXXXXXXXXX
29	0.90	11	XXXXXXXXXXX ←
30	0.95	11	XXXXXXXXXXX
31	1.00	5	XXXXX
32	1.05	5	XXXXX
33	1.10	5	XXXXX
34	1.15	8	XXXXXXXX
35	1.20	8	XXXXXXXX
36	1.25	7	XXXXXXX ←
37	1.30	6	XXXXXX
38	1.35	2	XX
39	1.40	2	XX
40	1.45	0	
41	1.50	0	
42	1.55	0	
43	1.60	0	
44	1.65	0	
45	1.70	0	
46	1.75	0	
47	1.80	0	
48	1.85	0	
49	1.90	0	
50	1.95	0	

STATION GROUPING

Bin Index											
1											
2											
3											
4											
5											
6											
7											
8											
9											
10											
11											
12											
13											
14											
15	3										
16	3										
17	3										
18	3	8	10								
19	4	6	7	8	10						
20	4	5	6	7	8	10					
21	4	5	6	7	8	9	10				
22	1	2	4	5	6	7	9				
23	1	2	5	9							
24	1	2	9								
25	1	2	19								
26	15	19									
27	12	15	18	19	20	21	22	23			
28	11	12	13	14	15	18	19	20	21	22	23
29	11	12	13	14	15	17	18	20	21	22	23
30	11	12	13	14	16	17	18	20	21	22	23
31	11	13	14	16	17						
32	16	17	24	31	32						
33	16	24	30	31	32						
34	24	26	27	29	30	31	32	33			
35	24	26	27	29	30	31	32	33			
36	25	26	27	28	29	30	33				
37	25	26	27	28	29	33					
38	25	28									
39	25	28									
40											
41											
42											
43											
44											
45											
46											
47											
48											
49											
50											

FIGURE S-6

HISTOGRAMS OF STATION NOISE LEVELS BY $\overline{N}$, BIN SIZE = 0.200;
75% OVERLAP, $\overline{N}$ = N - mB, WHERE m = 1.00

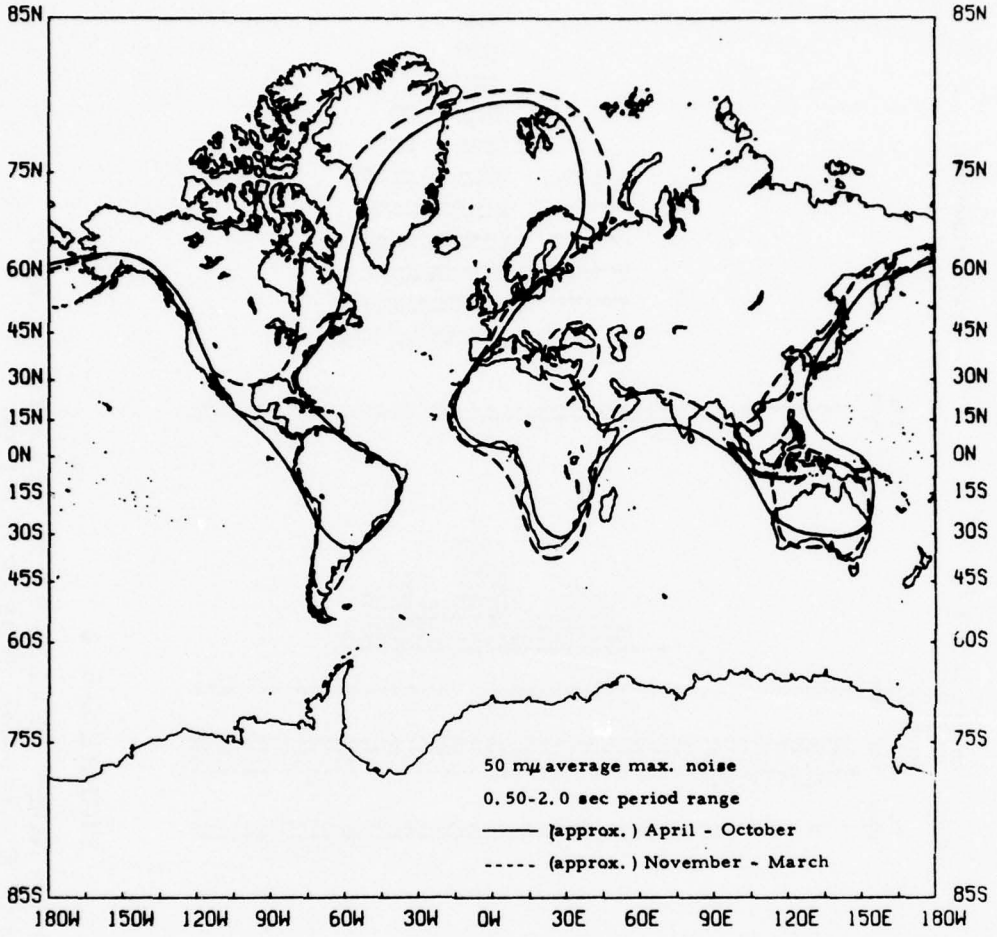

FIGURE S-7

SEASONAL EXTREMES OF 50 mμ NOISE CONTOUR

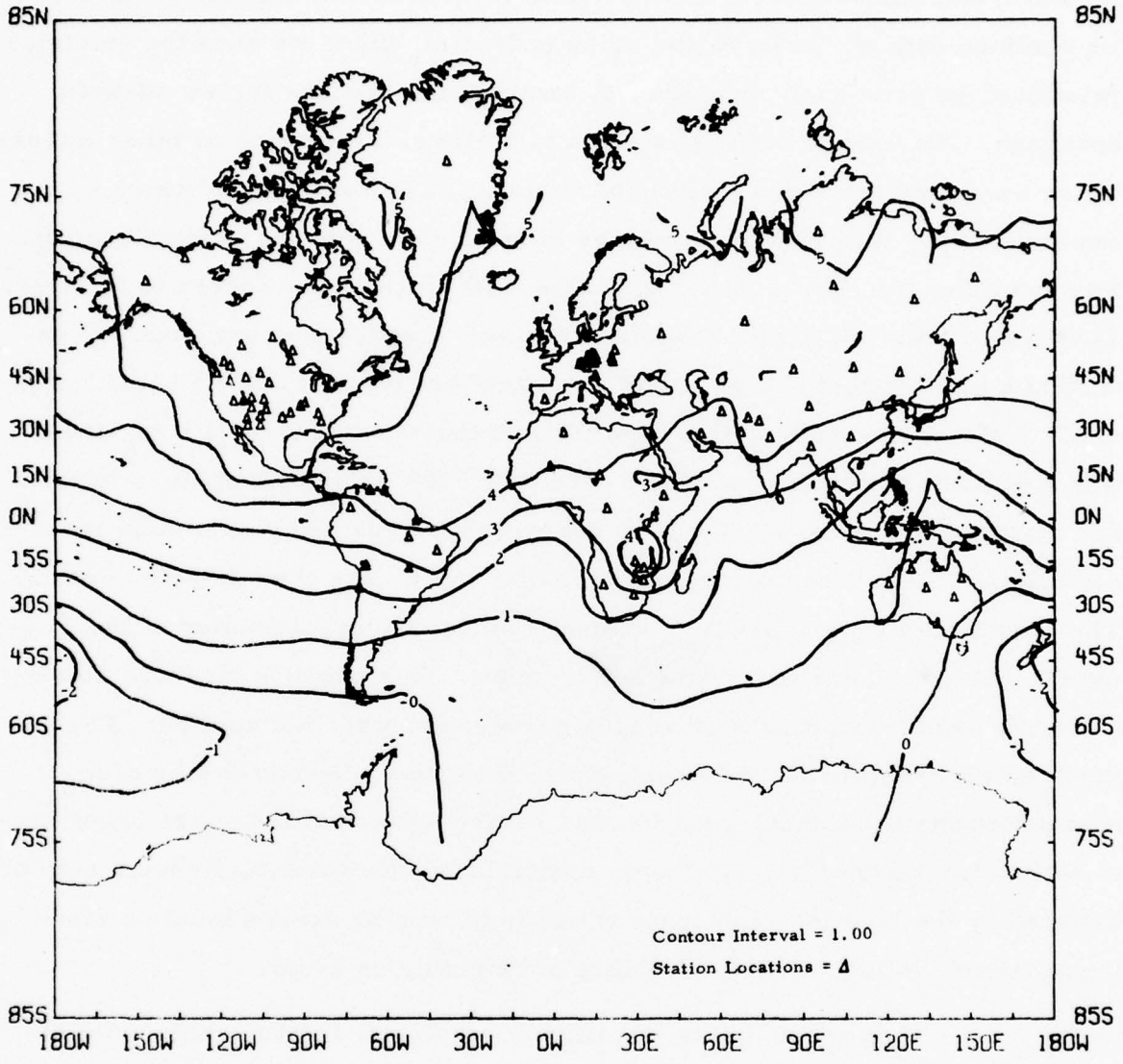

FIGURE S-8

LOG ($P_D/(1-P_D)$) OF DETECTION PROBABILITY FOR ARRAY-MODIFIED NETWORK ($m_b = 4.0$)

Network) and LRSM (Long-Range Seismic Measurement) stations from which we obtained data on short-period noise and/or m_b bias, we used the empirical relationships previously described to locate other stations for world-wide coverage. No consideration was given to political boundaries or other factors which are important for the siting of stations. The contours indicate, by the exponent of 10, the ratio of successes to failures in detecting seismic events. For example, the -1- contour indicates a 10^1 ratio of successes to failures. That contour and the higher contours indicate that the success ratio for detecting a hypothetical 4.0 m_b event was excellent for most of the earth. Figure S-9 shows that the location capability of the network for a 4.0 m_b event was a 95% confidence error ellipse less than 5000 square kilometers in area for most of the earth. Figure S-10 contours the expected bias of network estimates of m_b, based on averaging station m_b biases over detected events. The bias tended toward negative values, that is, under-estimates of the magnitude; but are less than 0.1 magnitude units. This network bias was obtained on the assumption that station bias corrections were not applied. For much smaller networks, we would expect the effect of network bias of m_b measurements to be much greater, the reason being that there are fewer stations to average down the effects of station bias. Network bias should also be affected by the locations and types of stations, and by source location since these factors influence the probability of detecting an event.

We conclude that significant empirical relationships exist between seismic noise and magnitude bias. These relationships can be used as a basis for zoning noise levels over large regions of the earth, and can thus with some precision predict the performance of good quality seismic stations prior to their installation. The weakness of this approach is the lack of sufficient data to accurately determine the boundaries of the seismic noise zones. With the use of other geophysical and geological information, such as gravity; heat flow; sedimentary, crustal, and upper mantle structure; it might be possible to more accurately define the boundary of seismic noise zones. Past

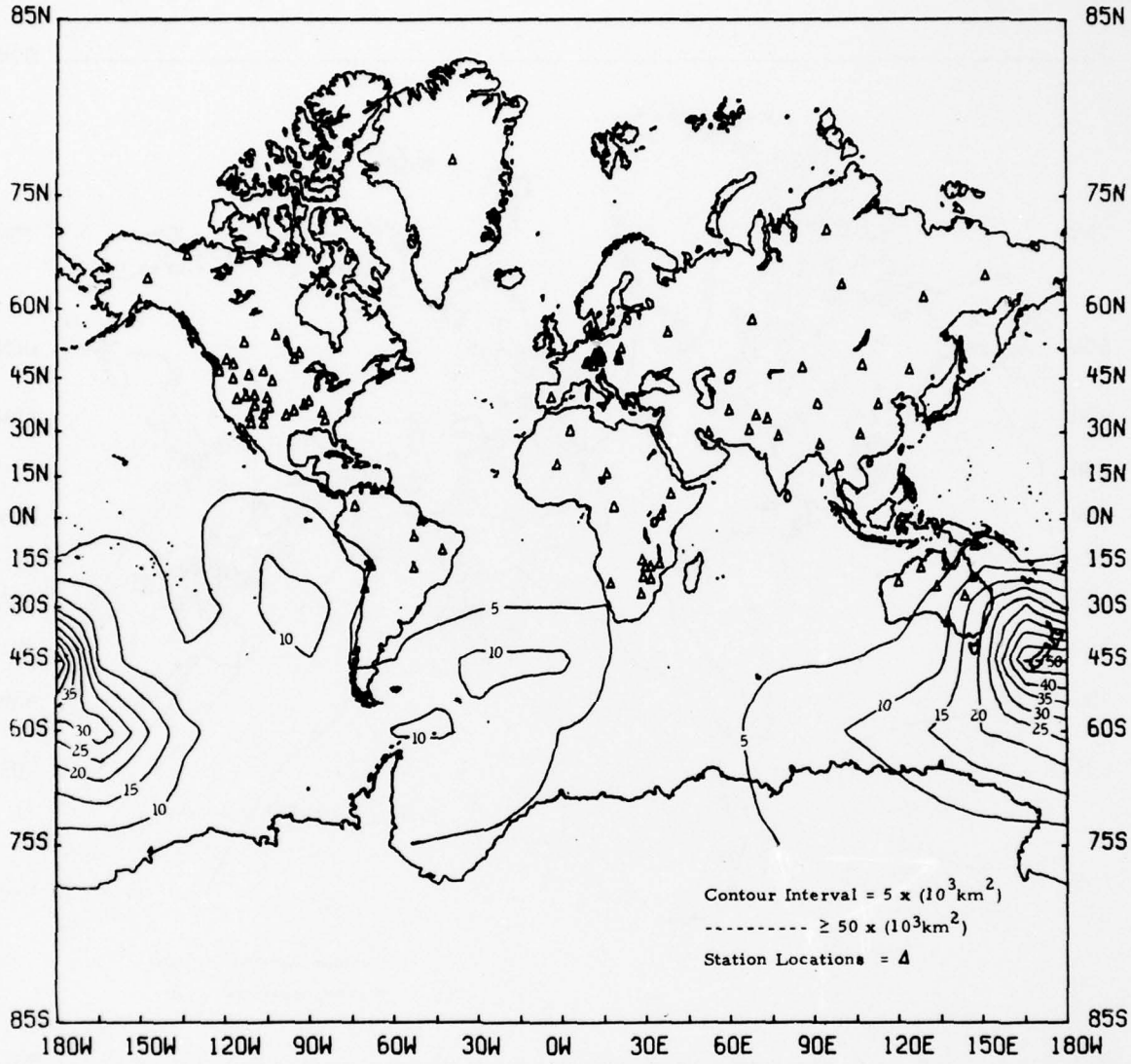

FIGURE S-9

95% ERROR ELLIPSE AREAS FOR ARRAY-MODIFIED NETWORK
(m_b = 4.0)

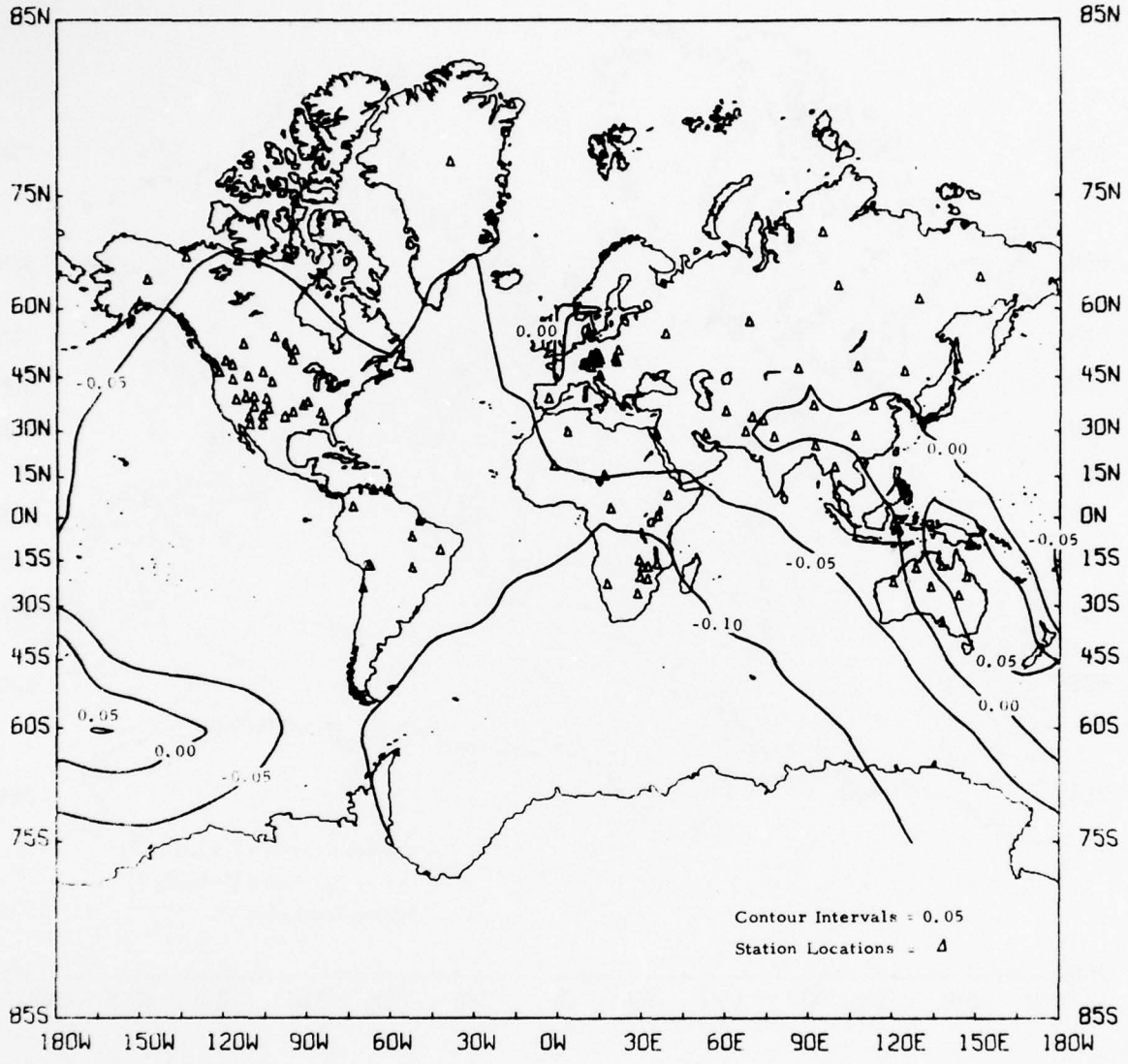

FIGURE S-10

AVERAGE NETWORK BIAS FOR ARRAY-MODIFIED NETWORK
(m_b = 4.0)

studies have suggested that the seismic wave mode structure of noise as determined from earth structures could be used to evaluate the effects of seismic structure on relative noise excitation. It would greatly enhance our approach toward predicting the optimum location of seismic sites, if such associated geophysical and geological information could be applied to the problem of estimating and delineating the boundaries of seismic noise zones.

The physical significance of our result is that it appears to support the hypothesis that mantle P-waves may be a dominant component of ambient seismic noise. This is consistent with the observation of mantle P-waves between 0.4 Hz and 1.2 Hz at the normally quiet Tonto Forest Observation (TFO) array site and of short-period noise during periods of elevated microseismic activity at the much noisier Large Aperture Seismic Array (LASA) in Montana. In both cases, the P-wave noise was observed to propagate from low-pressure zones simultaneously occurring over the Labrador Sea and Pacific Ocean. Rayleigh waves were also observed at the quiet TFO site but as predominantly diffuse wavenumber peaks isotropically distributed and also as a steady but much weaker peak associated with the Pacific low-pressure zone. Network studies of ambient noise at other noisier horizontal array sites such as the Cumberland Plateau Observatory (CPO) indicate that the noise is 80 to 90% Rayleigh waves and 10 to 20% bodywaves with discrete propagating components variable in time due to the shifts in storm activity. These horizontal array observations are not inconsistent with deep-well noise observations made between 0.5 and 2.0 Hz in sedimentary structures. The deep-well observations indicate approximately 90% Rayleigh waves at the surface and an ambient level of P-waves observed at depths where Rayleigh wave mode noise components are attenuated. Since the mantle P-waves extend several hundred kilometers into the earth, it is expected that the total energy of the mantle P-waves is at least an order of magnitude greater than the Rayleigh wave components. Thus, the mantle P-wave component could be considered as a driving function and controlling factor in the level of noise at

sites of similar geological structure. As such, factors such as upper mantle absorption and velocity will have a similar influence on a station's ambient noise and m_b bias observations. This would account for the linear relationship observed between high-frequency seismic noise and m_b bias at stations of similar sedimentary structure. It also implies that discrete storm-propagated Rayleigh wave frequency-wavenumber peaks are a much smaller component of the total ambient Rayleigh wave noise field at a site than is the diffused isotropic Rayleigh wave component as was observed at TFO, and perhaps is also much smaller than the non-propagating Rayleigh wave component associated with secondary receiver-site scattering. The observation of several noise groups can possibly be explained as follows. The highest-noise sites may be due to ocean proximity especially at areas of extensive shallow shelf zones. The high-noise sites are those containing the more recent, less consolidated low-velocity sediments which are efficient scatterers of Rayleigh waves near the surface. The medium-noise sites are those containing older and more consolidated high-velocity sedimentary layers, and the low-noise sites are those containing igneous and metamorphic basement rocks at the surface with deeper crustal Rayleigh wave modes which distribute the Rayleigh wave noise more deeply within the Earth's crust. The noise level within a group is a function of the attenuation characteristics of the upper mantle under the station (i. e., how much the driving P-wave noise is attenuated). These hypotheses for the existence of several noise groups and the linear relationship between bias and noise within these groups are probably oversimplified. Proximity to major structural features such as mountain belts, island arcs, etc. may also be important factors in influencing the level of noise components propagating from fixed directions and intersecting the structures. Also, proximity of local factors such as swamps, glacial deposits, and cultural noise sources is another possible influence. Such diverse factors would probably cause variance from the mean noise levels associated with each noise group. The small standard deviations associated with the noise groups may

be due to the manner in which seismic observatory sites were selected. It would be expected that there would be more noise groups and the standard deviations would be much larger if the observatory sites were selected on a purely random basis.

The evidence presented in this report suggests that a simple basis exists for optimizing the selection of sites and estimating the detection performance of sites and networks. However, the results are based on analyzing the small number of sites where joint observations of noise and m_b bias were readily available. Assuming normal statistics, the noise groupings and linear noise-m_b bias relationship is considered significant at a 1% level of error. To assure that the result is not a random occurrence, it should be checked by performing noise analysis on as many stations as possible where m_b bias measurements are available. If it should turn out that Rayleigh wave components propagating from storms are the primary driving function of noise rather than mantle P-waves, it would be difficult indeed to see why any relationship should exist between high-frequency seismic noise and m_b bias. We don't think there now is sufficient data on noise theory and observation in the literature to definitely resolve what we now consider an open question concerning our results.

SECTION I
INTRODUCTION

The objective of this study is to evaluate seismic stations for possible relationships, if any, between magnitude bias, short-period noise, and tectonic structure. A report on world-wide station magnitude bias by North (1977) forms the basis for the present study. In addition to his data, several world-wide noise studies are used to obtain the noise data to be correlated, if possible, with magnitude bias data. As a result, a group of stations with known magnitude bias, noise values, and tectonic classification is obtained as a data base. Various statistical methods are employed to determine if there is a relationship between the parameters.

Three models have been developed in the course of this investigation. These can be used to assign values to additional stations scattered throughout the world. Using these station parameters in conjunction with the program NETPROB, which is based on the program NET2 (Snell, 1976) and NETWORTH (Wirth, 1970); a brief network capability study on short-period detection is done for two simulated networks. One network consists of 100 single-site stations, and the other network consists of 28 arrays and 72 single-site stations. In performing this simulation, the location of some stations and their parameters are taken from published data. In extending geographical coverage to other areas, bias and noise are estimated based on results of this study.

The data available are not entirely self-consistent and the quality of it varies. Nonetheless, it is still considered possible to reach useful conclusions on the basis of this data. In extracting magnitude bias and noise measurements from the literature, it was only possible to obtain

33 stations with fair quality measurements of both types of information and an additional 13 stations having noise measurements of questionable quality. This is not considered an adequate amount of data to perform powerful statistical tests. However, the data were statistically analyzed with the use of significance tests based on the number of degrees of freedom available, and where possible, conclusions were drawn as to the statistical significance of the results.

Although we will attempt to show an empirical relationship between noise levels and the magnitude bias, the plausibility of such a relationship is based on consideration of a possible physical basis for the relationship. Bradner et al. (1970) identified twenty organ pipe modes of ocean wave and associated seismic noise peaks between 0.02 and 5.0 Hz. The formation of these modes are implicit of a broadly distributed forcing function exciting spectral peaks characteristic of the local bathymetry and are consistent with the theories of Longuet-Higgins (1950) and Hasselman (1963) for generating seismic waves from ocean waves. Dinger (1963) and Haubrich and McCamy (1969) observed time delays and dispersion consistent with the generation of seismic waves from ocean-storm gravity waves interacting at the coastline nearest to the seismic station. Toksöz and Lacoss (1968), analyzing microseisms at the LASA array station during periods of relatively high microseismic activity, associated strong coherent mantle P-wave peaks between 0.4 Hz and 0.6 Hz with broad low-pressure areas simultaneously located in the Labrador Sea and the Pacific Ocean. Binder and Burg (1967) and Burg and Burrell (1967) also observed P-wave noise between 0.4 and 1.2 Hz associated with broad low-pressure areas simultaneously occurring in the Labrador Sea and the Pacific Ocean in data from the very quiet TFO array station. Rayleigh waves were also observed at levels 4 to 5 dB lower than the P-wave noise spectrum. At more typical noisier sites, Johnson et al. (1966) observed the noise at the Earth's surface to consist of 80 to 90% Rayleigh waves and 10 to 20% mantle P-waves. Johnson et al. also observed that most of the Rayleigh

wave noise at the CPO array was isotropic, which is consistent with receiver-site scattering as the mechanism for generating high-frequency Rayleigh wave noise. Douze (1967) observed at a number of deep-well noise observations that both surface waves and mantle P-waves occur in the ambient seismic noise between 0.5 and 2.0 Hz. In the same frequency range, Sax (1965) showed that all surface wave modes were exicted with approximately the same total energy, suggesting the importance of receiver-site scattering as the mechanism for generating the Rayleigh wave noise. That model also predicted that at sites with sedimentary layers, the noise at the surface can be expected to contain about 90% fundamental mode Rayleigh waves. Capon (1973) analyzing noise data from the ALPA and NORSAR array site indicated that noise between 0.5 Hz and 2.0 Hz consisted of a large non-propagating component (e.g., receiver-site scattering) and that propagating Rayleigh wave components were observed to be highly diffused in wavenumber space (e.g., isotropic). Sax (1970) examining noise from a quiet three-dimensional array site, observed that the P-wave noise steered to the location of earthquakes completely dominated the noise, suggesting that the ambient P-wave component is a world-wide ocean-generated phenomena, whereas storms are associated with P-wave noise elevated above an ambient steady-state level.

SECTION II
BACKGROUND

North (1977) analyzed 400,000 station m_b values as reported in the International Seismological Center (ISC) bulletins to determine station magnitude biases, defined as the mean difference between station m_b and average m_b of a large network of stations, and their causes and effects. He found that although there are clear indications that the biases are functions of both source region and time, they appear to be well correlated with tectonic structure and lateral variations of attenuation characteristics in the upper mantle under the station. Analysis showed that the station biases were highest (attenuation lowest) in shield regions such as Canada, India, and Scandinavia and were lowest (attenuation highest) in east Africa rift zones and the western United States, which has upper mantle characteristics similar to a rift zone.

Application of the station biases as station m_b corrections for a given event reduces the scatter in m_b measurements ($m_b \geq 4.0$) and also removes many of the apparent changes with time in the magnitude distribution curve introduced by temporal changes of the distribution of stations. Table II-1 summarizes North's conclusions.

TABLE II-1

MAGNITUDE BIAS

$b_{ij} = m_{ij} - m_j$ where m_{ij} = i^{th} station m_b of j^{th} event.

m_j = event $m_b = \frac{1}{N} \sum_{i=1}^{N} m_{ij}$ N = # of stations reporting

$N_{min} = 15$

Conclusions of North (1977):

- Bias is well correlated with the tectonic structure and lateral variations in attenuation characteristics of the upper mantle under the station.
- Indications were obtained that station magnitude bias is a function of source region; it was also observed to vary with time; the exact relationships determining the bias are not yet completely resolved.
- Application of the station biases as station m_b corrections reduced the scatter in m_b observations for a single event (above $m_b = 4.0$).
- Station m_b corrections greatly reduced the temporal variation of seismicity introduced by the change in station distribution with time.

SECTION III
DATA COLLECTION

A data base of 33 stations, where the bias, noise, and tectonic type are known, is used to establish a relationship between the three parameters. Thirteen additional stations with slightly questionable noise values are added later to increase the data base and to further test the relationship established by using the 33 original stations. Although the instrumentation and installation of the stations differ, an attempt has still been made to determine any significant relationships which can be developed on the basis of these data. Hopefully, any relationship observed will be independent of the type of station.

The magnitude biases and tectonic types of the majority of stations were obtained from North (1977), and additional bias values were obtained from Evernden and Kohler (1976). In order to obtain bias figures from the report by Evernden and Kohler, station EUR of North's report was considered equivalent to station EKNV of the report by Evernden and Kohler since the locations are approximately the same (Eureka, Nevada). This station will be referred to as EUR in later station listings. The tectonic classification of BUL has been changed from rift to shield after referencing a tectonic map of the world in Smith (1973).

The noise values for the original stations have been obtained from Fix, Swanson, and Ballard (1973); and Evernden and Kohler (1976). These noise values are used as $\log_{10}$ of the peak-to-peak amplitude and are considered fairly reliable. It should be noted that CPO and UBO are arrays, and therefore the noise values are somewhat lower than might otherwise be expected. The noise values for the 13 additional stations have been obtained from the noise study by Hair, Funk, and Research Staff (1964). These noise

values are considered questionable because the exact type of measurement (i.e., zero-to-peak or peak-to-peak) could not be determined.

The noise means of these 13 additional stations and of the 33 original stations were compared using a two-sided Student's t-test. This test is commonly used for testing small samples ($N < 30$). The purpose of the significance test used in this study is to show if there is sufficient statistical evidence to reject the hypothesis that the means of two samples are equal. It was assumed that the population variance of the two samples are equal. In this application, a test-statistic is computed by dividing the difference between the two population means by a modified standard deviation which incorporates the standard deviation and size of both sample populations. This test statistic is then compared to a critical value obtained from a table of the cumulative t-distribution on the basis of the significance level desired and the number of degrees of freedom that exist for a given test. The null hypothesis is rejected if a positive test statistic is greater than or equal to the critical value or if a negative test statistic is less than or equal to the negative of the critical value (Ostle, 1963). In this case, the test was conducted with a significance level of 0.05. The results showed that the hypothesis that both sample means are equal cannot be rejected at this significance level. This outcome shows that it is statistically valid to consider the 13 additional stations to be equivalent to the original sample of 33 stations.

Both the bias and noise values for Long-Range Seismic Measurement (LRSM) stations RTNM, BXUT, LCNM, BLWV, BRPA, LSNH, RKON, and EBMT have been obtained from Evernden and Kohler (1976). Comparison of their values with those in LRSM reports by the Geotechnical Corporation (1965) and Pena (1967) has shown that the noise values for RKON and EBMT differ by a factor of 10; the values in the LRSM reports are used in this study. Table III-1 shows the stations, the station types, and the values and sources for their respective parameters. Figure III-1 shows the geographic distribution of the station locations.

A correction is applied to the noise values of stations within 500 km of the coast in order to remove the majority of the ocean noise. The correction is based on an empirical function derived by Griffin (1963), shown in Figure III-2. The constants used in Griffin's model were obtained for a profile perpendicular to the eastern United States seaboard. Beyond 100 km the relative decrease in amplitude is nearly the same at all frequencies. In the present study, a frequency of 0.25 Hz, the peak power frequency for noise in a short-period instrument, is used in the correction. Noise of other frequencies is assumed to be produced by scattering. The approximate distance, in 50 km steps, from the coast has been obtained from measurements on a map in the noise study by Hair, Funk, and Research Staff (1964). The actual correction is the $\log_{10}$ of the ratio of the relative noise at 500 km to the relative noise at the distance in question, the noise being normalized to the coast. Table III-2 shows the corrections used in this study. Application of these corrections results in the formation of another data set containing the noise values corrected for ocean noise.

TABLE III-1

DATA BASE STATIONS
(PAGE 1 OF 3)

Noise values are given in Log_{10}(peak-to-peak) (p-p).

Source Key for Station Lists

A	North (1977)
B	Everinden and Kohler (1976)
C	The Geotechnical Corporation (1965)
D	Fix, Swanson, and Ballard (1973)
E	Hair, Funk, and Research Staff (1964)
F	Line Model
G	Tectonic-Noise Group Model
H	Tectonic Model
I	National Earthquake Information Center (1970)
J	The Geotechnical Corporation (1964)
K	Approximate
L	Personal communication, Chang, A.C.

Tectonic Types

R	Rift zone; or region with similar upper mantle structure
P/F	Platform and fold belts
S	Shield
**	Station added to original data base of 33 stations
△	World-wide Standard Seismograph Network (WWSSN) Station
▲	Long-range Seismic Measurement (LRSM) Station
□	Canadian Network Seismograph Station
■	VELA array

Noise Groups (to be explained later in text)

1	Low
2	Medium
3	High
4	Very High (coastal)

TABLE III-1

DATA BASE STATIONS
(PAGE 2 OF 3)

Name	Latitude	Longitude	Tectonic Type	Grouping for Observed Noise	Grouping for Corrected Noise	Bias	Observed Noise	Corrected Noise	Source		
									Bias	Noise	Location
▲ BXUT	37.563 N	109.435 W	R	1	1	-0.18	0.43	0.43	B	B	L
▲ LCNM	32.402 N	106.599 W	R	2	2	-0.17	0.70	0.70	B	B	J
▲ EUR	39.483 N	115.970 W	R	1	1	-0.24	0.40	0.40	A	B	I
△ DUG	40.195 N	112.813 W	R	1	1	-0.15	0.398	0.398	A	B	I
△ BOZ	45.600 N	111.633 W	R	1	1	-0.06	0.398	0.398	A	B	I
■ UBO	40.322 N	109.569 W	R	1	1	-0.11	0.176	0.176	A	B	I
△ ALQ	34.942 N	106.459 W	R	2	2	-0.20	0.710	0.710	A	B	I
△ GOL **	39.700 N	105.371 W	R	2	2	-0.28	0.699	0.699	A	E	I
△ LON **	46.750 N	121.810 W	R	3	2	-0.30	0.954	0.742	A	E	I
△ TUC **	32.310 N	110.782 W	R	1	1	-0.14	0.477	0.317	A	E	I
■ CPO	35.595 N	85.570 W	P/F	1	1	-0.07	0.398	0.398	A	B	I
△ KBL	34.541 N	69.043 E	P/F	1	1	0.09	0.562	0.562	A	D	I
△ SHL	25.567 N	91.883 E	P/F	1	1	0.11	0.683	0.523	A	D	I
△ STU **	48.771 N	9.193 E	P/F	1	1	0.29	0.845	0.793	A	E	I
△ RAB **	4.191 S	152.170 E	P/F	2	1	0.12	1.176	0.804	A	E	I
△ COL	64.900 N	147.793 W	P/F	2	2	0.01	0.990	0.938	A	D	I
△ LPS	14.292 N	89.162 W	P/F	3	2	0.04	1.363	0.991	A	D	I
△ COP **	55.683 N	12.433 E	P/F	3	2	0.36	1.531	1.159	A	E	I
△ FLO **	38.802 N	90.370 W	P/F	2	2	0.26	1.255	1.255	A	E	I
△ CAR **	10.507 N	66.928 W	P/F	3	2	0.13	1.342	0.970	A	E	I
△ TRN **	10.649 N	61.403 W	P/F	4	2	0.07	1.491	1.119	A	E	I
▲ BRPA	39.925 N	78.844 W	P/F	2	2	0.06	1.00	1.00	B	B	J
▲ RTNM	36.729 N	104.361 W	P/F	2	2	0.09	0.90	0.90	B	B	J
▲ LSNH	44.238 N	71.923 W	P/F	3	2	0.00	1.30	1.02	B	B	J
△ PMG	9.409 S	147.154 E	P/F	3	2	0.10	1.366	0.994	A	D	I

TABLE III-1

DATA BASE STATIONS
(PAGE 3 OF 3)

Name	Latitude	Longitude	Tectonic Type	Grouping for Observed Noise	Grouping for Corrected Noise	Bias	Observed Noise	Corrected Noise	Source		
									Bias	Noise	Location
△ LPB	16.533 S	68.098 W	P/F	3	3	0.07	1.318	1.203	A	D	I
▲ BLWV	37.800 N	81.311 W	P/F	3	3	0.12	1.45	1.45	B	B	J
△ BKS **	37.877 N	122.235 W	P/F	4	3	0.18	1.763	1.391	A	E	I
△ RIV **	33.829 S	151.158 E	P/F	4	3	0.31	2.049	1.677	A	E	I
▲ EBMT	49.628 N	95.622 W	S	1	1	0.12	0.716	0.716	B	C	L
▲ RKON	50.839 N	93.672 W	S	1	1	0.28	0.716	0.716	B	C	J
□ RES **	74.687 N	94.900 W	S	1	1	0.13	0.000	0.000	A	E	I
□ ALE**	82.483 N	62.400 W	S	1	1	-0.04	0.477	0.105	A	E	I
△ NDI	28.683 N	77.217 E	S	2	2	0.33	1.109	1.109	A	D	I
△ NOR	81.600 N	16.683 W	S	3	2	-0.14	1.102	0.730	A	D	I
△ KON	59.649 N	9.632 E	S	3	2	0.07	1.318	0.946	A	D	I
△ KOD	10.233 N	77.467 E	S	3	2	0.06	1.329	0.957	A	D	I
△ NUR	60.509 N	24.651 E	S	3	2	0.19	1.443	1.071	A	D	I
△ BUL	20.143 S	28.613 E	S	3	3	-0.07	1.134	1.134	A	D	I
△ WIN	22.567 S	17.100 E	S	4	3	-0.09	1.331	1.119	A	D	I
△ PRE	25.753 S	28.190 E	S	4	3	-0.07	1.331	1.279	A	D	I
△ GDH	69.250 N	53.533 W	S	4	3	0.00	1.575	1.203	A	D	I
△ KEV	69.755 N	27.007 E	S	4	3	0.02	1.559	1.187	A	D	I
△ MUN	31.978 S	116.208 E	S	4	3	0.15	1.637	1.265	A	D	I
△ POO	18.533 N	73.850 E	S	4	3	0.17	1.643	1.271	A	D	I
△ KTG	70.417 N	21.983 W	S	4	3	0.02	1.628	1.256	A	D	I

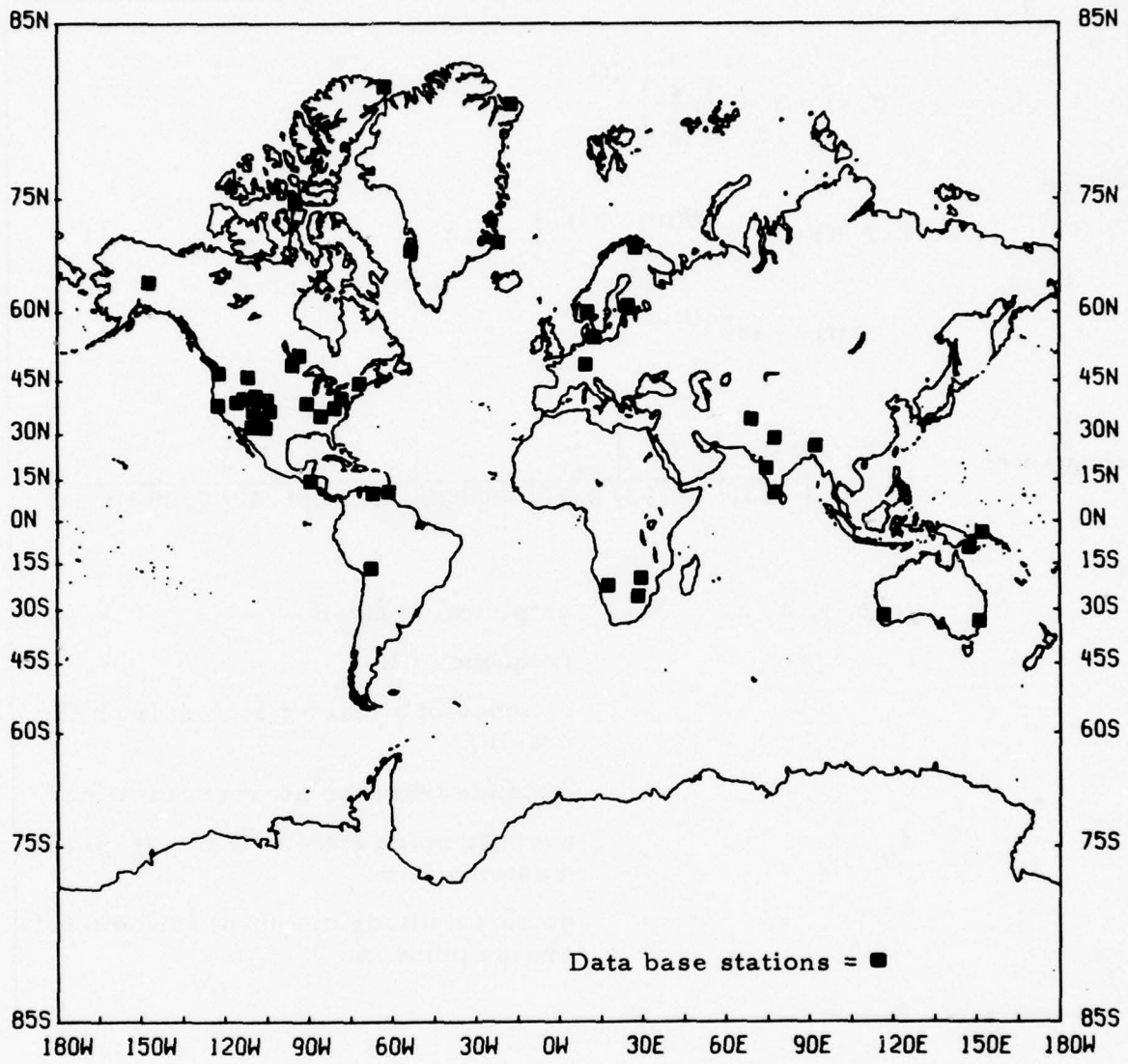

FIGURE III-1

GEOGRAPHIC DISTRIBUTION OF DATA BASE STATION LOCATIONS

$$Y(f,x) = Y_o(f)\left[\frac{x}{x_o}\right]^{k(f)}$$

where

$$\ln Y_o(f) = \left[\alpha e^{-\beta(\ln(f/\gamma))^2}\right] - \ln 50$$

$$k(f) = a e^{-b(\ln(f/c))^2}$$

constants:

x_o	α	β	γ	a	b	c	f
350 km	7.61	0.382	0.20	-0.878	0.169	1.40	0.25 Hz

α, β, γ, a, b, c	empirical constants
f	frequency (Hz)
x_o	distance of a master station from the coastline
x	distance from the nearest coastline
Y_o	average noise amplitude mμ (p-p) at master station
Y	noise amplitude mμ (p-p) at some reference point, x.

FIGURE III-2

BASIS CF NOISE CORRECTION FOR COASTLINE PROXIMITY
GRIFFIN (1963)

TABLE III-2

NOISE CORRECTIONS

Distance From Coast	Additive Correction $\text{Log}_{10}\left(\frac{\text{relative noise at 500 km}}{\text{relative noise at station distance}}\right)$
≤100 km	-0.372
150 km	-0.279
200 km	-0.212
250 km	-0.160
300 km	-0.118
350 km	-0.083
400 km	-0.052
450 km	-0.024
≥500 km	0.000

SECTION IV

GROUPING OF NOISE DATA BASED ON AN EMPIRICAL RELATIONSHIP BETWEEN NOISE AMPLITUDE AND MAGNITUDE BIAS

Two sets of data, one with observed noise and the other with corrected noise, have been processed to determine if any grouping of the noise values ($\log_{10}$ peak-to-peak) exists. Similarities exist between magnitude bias and noise amplitude in that both are affected by attenuation in the same manner. Since high (positive) bias implies low attenuation (high signal amplitude) and low (negative) bias implies high attenuation (low signal amplitude), the noise in these cases should also be high and low, respectively. This similarity led to the decision to search for a linear relationship between bias and noise. The objective of this search originally was to develop a relationship by which noise could be computed from bias. The processing was done on the basis of $\bar{N}$, where $\bar{N} = N - mB$, and where N is the noise, B is the magnitude bias, and m is the slope. A set of slopes ranging from 0.25 to 0.5 in 0.05 increments and from 0.50 to 5.00 in 0.10 increments was examined to determine if any grouping of the $\bar{N}$'s for each station into subsets occurred. Histograms such as those shown in Figure IV-1 were generated for this set of slopes and were visually examined to determine which slopes showed the most promising grouping into subsets. Several slopes were selected in this manner and then subset groupings were further examined. The standard deviation of $\bar{N}$'s from the lines of the selected subset groupings was also determined for cases where the lines for each subset were defined using constrained slopes and least-square slopes.

It was found that several different subset groupings of $\bar{N}$ were feasible interpretations, the standard deviations obtained for the selected representations being similar. For the data used in this study, the representations with subsets defined by least-square estimated slopes, and those

A. 33 STATIONS WITH OBSERVED NOISE

STATION VALUES

m = 1.00

I	Name	Bias	Noise	$\bar{N}$
1	EUR	-0.240	0.400	0.640
2	BRUT	-0.180	0.430	0.610
3	UBO	-0.110	0.176	0.286
4	BOZ	-0.060	0.398	0.458
5	DUG	-0.150	0.398	0.589
6	CPO	-0.070	0.399	0.469
7	KBI	0.090	0.562	0.472
8	SWL	0.110	0.683	0.573
9	EBRT	0.120	0.716	0.596
10	RKON	0.280	0.716	0.436
11	ALQ	-0.200	0.710	0.910
12	LCMF	-0.170	0.700	0.870
13	COL	0.010	0.990	0.980
14	BPPA	0.060	1.000	0.940
15	RTNH	0.090	0.900	0.810
16	NDI	0.330	1.109	0.779
17	LSNR	0.0	1.300	1.300
18	LPS	0.040	1.363	1.323
19	PNG	0.100	1.366	1.266
20	LPB	0.070	1.253	1.183
21	BLWV	0.120	1.450	1.330
22	MOR	-0.180	1.102	1.282
23	KON	0.070	1.318	1.248
24	KOD	0.060	1.329	1.269
25	BWL	-0.070	1.134	1.204
26	HUP	0.190	1.443	1.253
27	WIH	-0.090	1.331	1.421
28	PRZ	-0.070	1.331	1.401
29	GDH	0.0	1.575	1.575
30	KEV	0.020	1.559	1.539
31	HWN	0.150	1.637	1.487
32	POO	0.170	1.643	1.473
33	KTG	0.020	1.628	1.608

Noise Groups		Stations
	1 Low	1-10
	2 Medium	11-16
	3 High	17-26
	4 Very High (Coastal)	27-33

HISTOGRAM OF $\bar{N}$

Bin Index	Center $\bar{N}$ of Bin	# in Bin	
1	-0.50	0	
2	-0.45	0	
3	-0.40	0	
4	-0.35	0	
5	-0.30	0	
6	-0.25	0	
7	-0.20	0	
8	-0.15	0	
9	-0.10	0	
10	-0.05	0	
11	0.00	0	
12	0.05	0	
13	0.10	0	
14	0.15	0	
15	0.20	1	X
16	0.25	1	X
17	0.30	1	X
18	0.35	2	XX
19	0.40	5	XXXXX
20	0.45	5	XXXXX
21	0.50	7	XXXXXXX
22	0.55	8	XXXXXXXX
23	0.60	5	XXXXX
24	0.65	4	XXXX
25	0.70	3	XXX
26	0.75	2	XX
27	0.80	3	XXX
28	0.85	5	XXXXX
29	0.90	5	XXXXX
30	0.95	4	XXXX
31	1.00	3	XXX
32	1.05	1	X
33	1.10	1	X
34	1.15	4	XXXX
35	1.20	7	XXXXXXX
36	1.25	10	XXXXXXXXXX
37	1.30	9	XXXXXXXXX
38	1.35	8	XXXXXXXX
39	1.40	7	XXXXXXX
40	1.45	5	XXXXX
41	1.50	6	XXXXXX
42	1.55	5	XXXXX
43	1.60	3	XXX
44	1.65	2	XX
45	1.70	1	X
46	1.75	0	
47	1.80	0	
48	1.85	0	
49	1.90	0	
50	1.95	0	

STATION GROUPING

Bin Index	
1	
2	
3	
4	
5	
6	
7	
8	
9	
10	
11	
12	
13	
14	
15	3
16	3
17	3
18	3 10
19	4 6 7 10
20	4 5 6 7 10
21	4 5 6 7 8 9 10
22	1 5 6 7 8 9
23	1 5 8 9
24	1 5 8 9
25	1 2 16
26	15 16
27	12 15 16
28	11 12 14 15 16
29	11 12 13 14 15
30	11 12 13 14
31	11 13 14
32	13
33	20
34	20 22 23 25
35	19 20 22 23 24 25 26
36	17 18 19 20 21 22 23 24 25 26
37	17 18 19 21 22 23 24 25 26
38	17 18 19 21 26 27 28
39	17 18 21 27 28 31 32
40	27 28 30 31 32
41	27 28 29 30 31 32
42	29 30 31 32 33
43	29 30 33
44	29 33
45	33
46	
47	
48	
49	
50	

FIGURE IV-1

HISTOGRAMS OF STATION NOISE LEVELS BY $\bar{N}$, BIN SIZE = 0.200;
75% OVERLAP, $\bar{N}$ = N - mB, WHERE m = 1.00
(PAGE 1 OF 2)

B. 33 STATIONS WITH NOISE CORRECTED FOR OCEAN NOISE

STATION VALUES

m = 1.00

I	Name	Bias	Noise	$\overline{N}$
1	EUR	-0.240	0.400	0.640
2	RKVT	-0.180	0.430	0.610
3	UBO	-0.110	0.176	0.286
4	BOZ	-0.060	0.398	0.458
5	DUG	-0.150	0.398	0.548
6	CPO	-0.070	0.398	0.468
7	KRL	0.090	0.562	0.472
8	SHL	0.110	0.523	0.413
9	EBMT	0.120	0.716	0.596
10	RKON	0.280	0.716	0.436
11	ALJ	-0.200	0.710	0.910
12	LCHM	-0.170	0.700	0.870
13	COL	0.010	0.938	0.928
14	BRBA	0.060	1.000	0.940
15	BTHM	0.090	0.900	0.810
16	LSHR	0.0	1.021	1.021
17	LPS	0.040	0.991	0.951
18	PMG	0.100	0.994	0.894
19	WDI	0.330	1.109	0.779
20	KON	0.070	0.946	0.876
21	KOD	0.060	0.957	0.897
22	NTR	0.190	1.071	0.881
23	NOR	-0.140	0.730	0.870
24	LPR	0.070	1.203	1.133
25	BLWV	0.120	1.450	1.330
26	BUL	-0.070	1.134	1.204
27	WIN	-0.090	1.119	1.209
28	PRE	-0.070	1.279	1.349
29	GDH	0.0	1.203	1.203
30	KEV	0.020	1.187	1.167
31	MUN	0.150	1.265	1.115
32	POO	0.170	1.271	1.101
33	KTG	0.020	1.256	1.236

Noise-Groups		Stations
	1 Low	1-10
	2 Medium	11-23
	3 High	24-33

HISTOGRAM OF $\overline{N}$

Bin Index	Center $\overline{N}$ of Bin	# in Bin	
1	-0.50	0	
2	-0.45	0	
3	-0.40	0	
4	-0.35	0	
5	-0.30	0	
6	-0.25	0	
7	-0.20	0	
8	-0.15	0	
9	-0.10	0	
10	-0.05	0	
11	0.00	0	
12	0.05	0	
13	0.10	0	
14	0.15	0	
15	0.20	1	X
16	0.25	1	X
17	0.30	1	X
18	0.35	3	XXX
19	0.40	5	XXXXX
20	0.45	6	XXXXXX
21	0.50	7	XXXXXXX
22	0.55	7	XXXXXXX
23	0.60	4	XXXX
24	0.65	3	XXX
25	0.70	3	XXX
26	0.75	2	XX
27	0.80	8	XXXXXXXX
28	0.85	11	XXXXXXXXXXX
29	0.90	11	XXXXXXXXXXX
30	0.95	11	XXXXXXXXXXX
31	1.00	5	XXXXX
32	1.05	5	XXXXX
33	1.10	5	XXXXX
34	1.15	8	XXXXXXXX
35	1.20	8	XXXXXXXX
36	1.25	7	XXXXXXX
37	1.30	6	XXXXXX
38	1.35	2	XX
39	1.40	2	XX
40	1.45	0	
41	1.50	0	
42	1.55	0	
43	1.60	0	
44	1.65	0	
45	1.70	0	
46	1.75	0	
47	1.80	0	
48	1.85	0	
49	1.90	0	
50	1.95	0	

STATION GROUPING

Bin Index											
1											
2											
3											
4											
5											
6											
7											
8											
9											
10											
11											
12											
13											
14											
15	3										
16	3										
17	3										
18	3	8	10								
19	4	6	7	8	10						
20	4	5	6	7	8	10					
21	4	5	6	7	8	9	10				
22	1	2	4	5	6	7	9				
23	1	2	5	9							
24	1	2	9								
25	1	2	19								
26	15	19									
27	12	15	18	19	20	21	22	23			
28	11	12	13	14	15	18	19	20	21	22	23
29	11	12	13	14	15	17	18	20	21	22	23
30	11	12	13	14	16	17	18	20	21	22	23
31	11	13	14	16	17						
32	16	17	24	31	32						
33	16	24	30	31	32						
34	24	26	27	29	30	31	32	33			
35	24	26	27	29	30	31	32	33			
36	25	26	27	28	29	30	33				
37	25	26	27	28	29	33					
38	25	28									
39	25	28									
40											
41											
42											
43											
44											
45											
46											
47											
48											
49											
50											

FIGURE IV-1

HISTOGRAMS OF STATION NOISE LEVELS BY $\overline{N}$, BIN SIZE = 0.200;
75% OVERLAP, $\overline{N}$ = N - mB, WHERE m = 1.00
(PAGE 2 OF 2)

defined by fixed slopes yield similar standard deviations. As fixing the slope, m in the above equation, allows more degrees of freedom, it turns out to be preferable over using least-squares to determine the slope. The results based on statistical tests of significance are improved by using a fixed slope, due to the larger number of degrees of freedom available for estimating the combined variance of data in all the groups of a given model.

A plot of relative signal amplitude (directly related to bias) versus noise amplitude (Evernden and Filson, 1971; Blandford and Sweetser, 1975) which was originally taken from Evernden and Clark (1970b) shows several linear relationships between these two parameters for different station geologies. The slope illustrated by the plot is the inverse of the slope defined in this study. Evernden and Filson (1971) in referring to this plot state that for granite or equivalent sites there is a linear relationship between log amplitude and log noise level such that a 10-fold change in noise level implies on the average a $2\frac{1}{2}$-fold change in P amplitude. The corresponding slope in this study would be approximately 2.50.

Upon investigation of various slopes, including a slope of 2.50, it was found that a slope of 1.00 was the best interpretation. Although other slopes had slightly lower standard deviations, they also involved additional groups and some included outliers. It was considered that the fewer were the number of groups, the more desirable was the interpretation. A slope of 1.00 gave the lowest standard deviation with a minimum number of groups, and accounted for all of the data. Using a slope of 1.00 to define the relationships also greatly simplifies interpretation.

The significance of a slope of 1.00 defining the relationship between noise magnitude and station magnitude bias, is that within each of the normal noise groups, neither noise nor bias is a controlling factor in optimum site selection. In this case, the goal of site selection is simply to find geographical locations of the quieter noise groups. Four distinct noise

levels were observed in the first data set examined. However, after correction of the noise for coastline proximity, this was reduced to three even more distinct groups. The highest noise group is eliminated by the application of the coastline correction to stations that are under 500 km from the coast. Although one noise group has been eliminated by this correction, after applying the correction, the average $\overline{N}$ values of the noise groups stay approximately the same. The stability of the grouping is thus shown in this manner. These results are illustrated by Figure IV-1.

The noise groups for each station are tabulated in Table III-1. Comparison of the groups with the station types shows that the grouping is independent of the types of station used. That is, a specific type of station is not confined to a specific noise group, except for the cases where the station type is represented by only a few stations.

Figures IV-2 show plots of log (p-p noise amplitude) versus m_b bias for all 46 stations and for the cases of both corrected and uncorrected noise. The lines shown in these figures represent the different noise level groups established using the original 33 stations. As can be seen in the figures for the observed noise values, the four noise groups are fairly well-defined. The three remaining noise groups are still apparent after application of the noise correction for coastline proximity. The 13 additional stations were added to the existing groups by computing the equivalent-zero-bias noise for each station (using a slope of 1.00) and assigning the station to the group having the closest average equivalent-zero-bias noise. As can be seen in the figure, the additional points follow the previously observed trends for the most part. The average equivalent-zero-bias noise levels for the various lines are not greatly affected by the addition of these points.

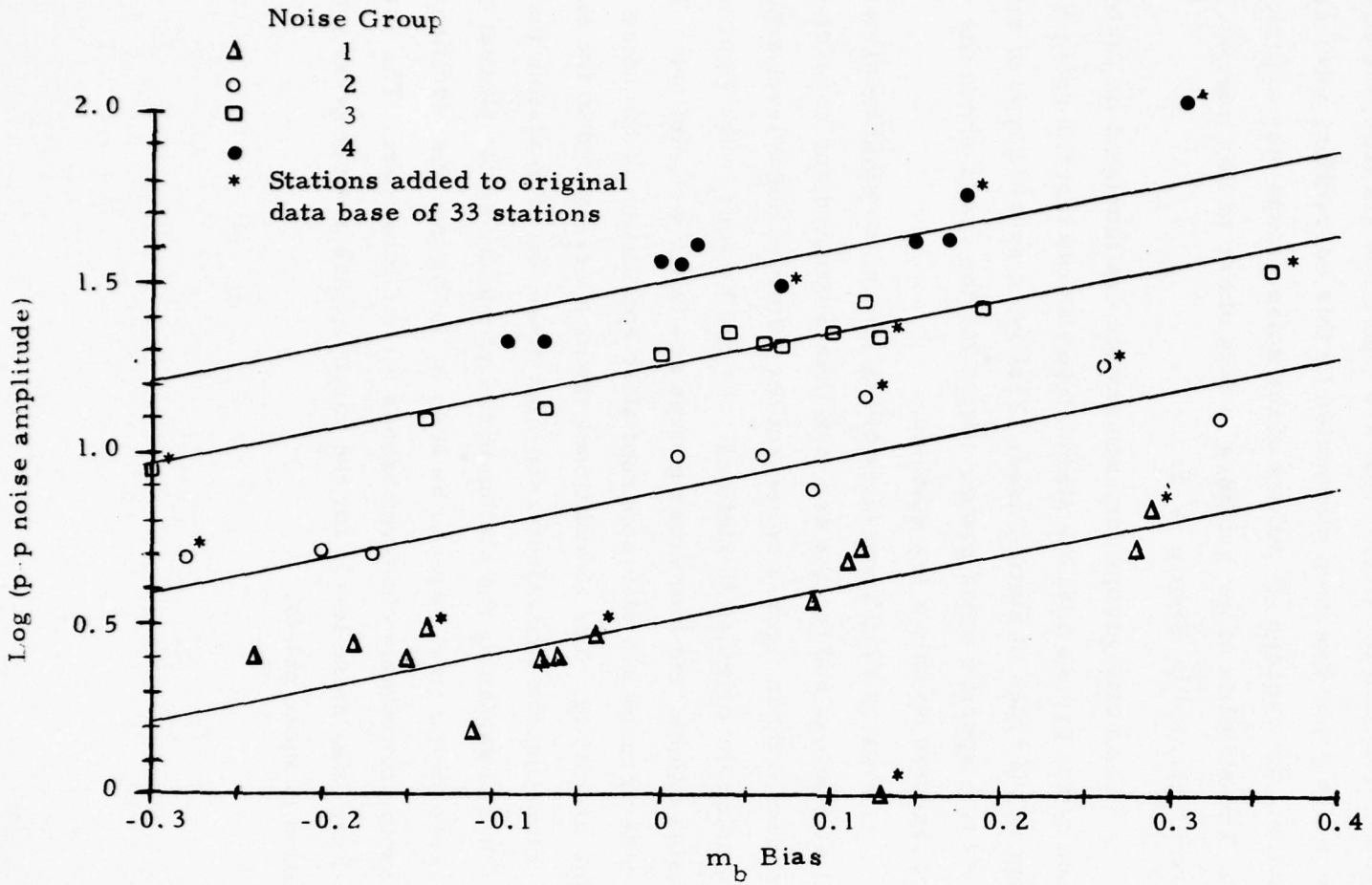

FIGURE IV-2A

LOG (p-p NOISE AMPLITUDE) VERSUS m_b BIAS FOR
46 STATIONS USING OBSERVED NOISE AMPLITUDES

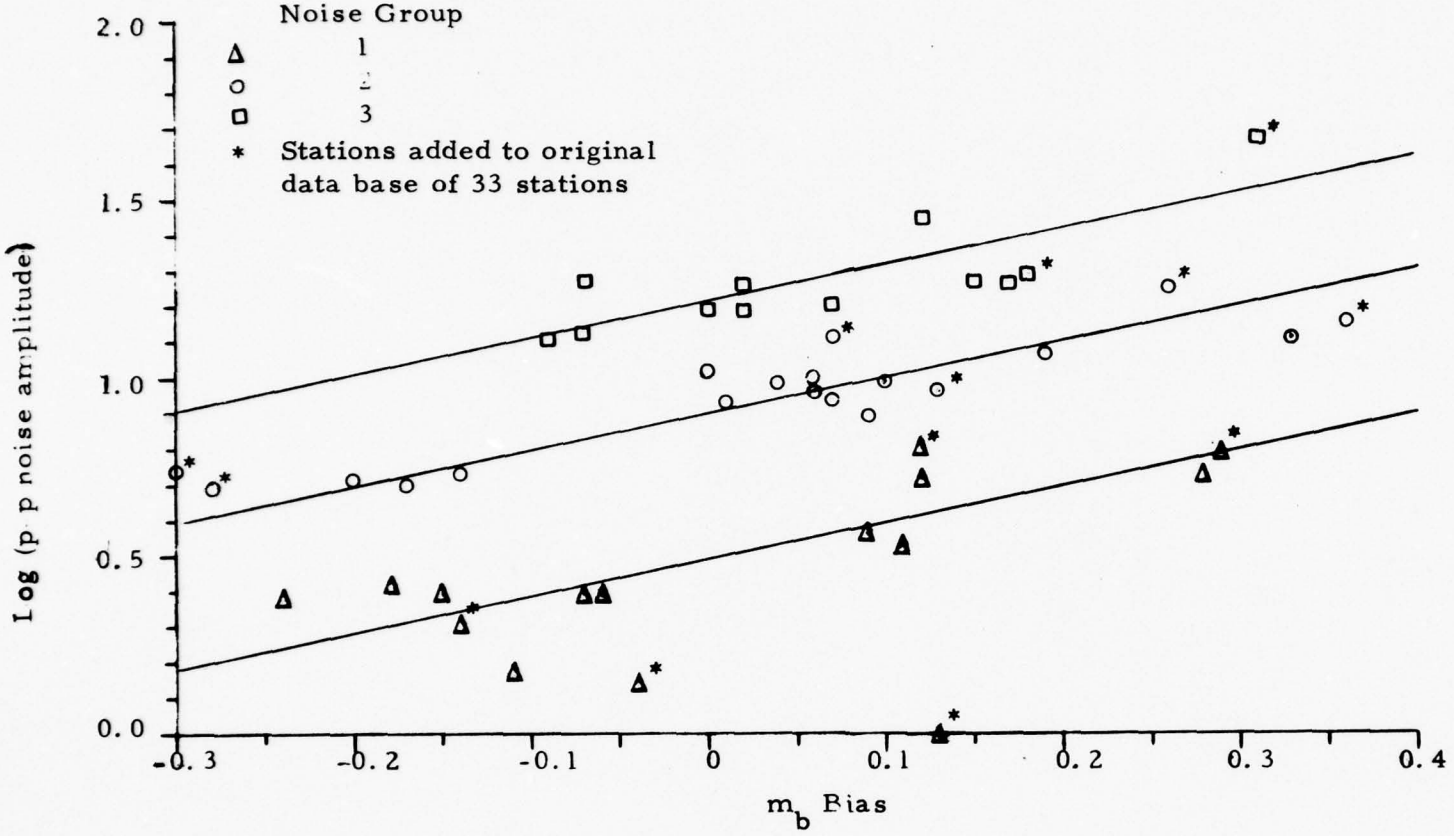

FIGURE IV-2B

LOG (p p NOISE AMPLITUDE) VERSUS m_b BIAS FOR
46 STATIONS USING NOISE AMPLITUDES CORRECTED FOR OCEAN NOISE

SECTION V

THE RELATIONSHIP BETWEEN NOISE GROUPS AND TECTONICS

It has been shown that seismic noise at stations can be described by a set of noise groups. The particular grouping illustrated by Figure IV-1 is based on a linear relationship (slope of one) between the noise magnitude, $\log_{10}$ (peak-to-peak), and the bias of magnitude measurements. Figure IV-1 shows that the grouping was sufficiently distinct to determine with little ambiguity the stations associated with each group. Large deviations of the assumed slope of the straight-line noise-bias relationship can be shown to make little or no change in the partitioning of stations between the distinct noise groups. In this section, the noise levels characterizing each group are given as intercept values of the noise which corresponds to zero bias in station magnitude measurement. The models were developed based on the original set of 33 stations for both the data set with observed noise and for the data set with noise corrected for coastline proximity as shown in Table III-2. An additional realization will be shown incorporating the 13 additional stations.

Part A of Table V-1 shows how the 33 stations are distributed with respect to noise measurements, and tectonic provinces. The first three rows of column 5 show the number of stations in each tectonic province. The first four columns of row 4 show the number of stations in each noise group. Row 4, column 5 shows the total number of stations considered. The general lack of a strong correlation between tectonic type and noise group can be seen in this table. In general,the rifts seem to be related to the low noise groups, platforms and folds to the intermediate noise groups, and shields to the high noise groups.

TABLE V-1

RELATIONSHIP BETWEEN NOISE LEVEL AND TECTONICS
(PAGE 1 OF 4)

Definition of indices indicating type of noise groups and tectonic types

j = 1 Low noise
2 Medium
3 High
4 Very high (coastal)
5 All above groups combined

k = 1 Rift
2 Platform or fold belt
3 Shield
4 All above groups combined

A. 33 Joint Classifications of Stations by Noise Zone and Tectonic Region

k \ j	1	2	3	4	5
1	5	2	0	0	7
2	3	3	5	0	11
3	2	1	5	7	15
4	10	6	10	7	33

Table entries represent the number of stations in each joint classification

B. Noise Prediction: Line Model

N_{jk}: Average noise magnitude $\log_{10}$(p-p) B_{jk}: Average P wave magnitude

$\overline{N}_{jk} = N_{jk} - B_{jk} + \text{Error}$ (error considered normal)

$\overline{N}_{jk}$:

k \ j	1	2	3	4
1	0.51	0.89	-	-
2	0.50	0.91	1.28	-
3	0.52	0.78	1.24	1.50
4	0.51	0.88	1.26	1.50

Error Standard Deviation:

j	1	2	3	4	5
B_{j4}	0.11	0.08	0.04	0.08	0.08
N_{j4}	0.11	0.08	0.04	0.08	0.08
df	9	5	9	6	29

Degrees of Freedom (df) for the standard deviations (S. D.) equal occurrences minus the number of parameters estimated times number of groups in which the parameters are estimated.

TABLE V-1

RELATIONSHIP BETWEEN NOISE LEVEL AND TECTONICS
(PAGE 2 OF 4)

C. Bias and Noise Prediction: Tectonic Model

Mean:

k	1	2	3
B_k	-0.16	0.06	0.07
N_k	0.46	1.02	1.31

Error Standard Deviation:

k	1	2	3	4
B_k	0.06	0.05	0.14	0.10
N_k	0.19	0.36	0.30	0.30

(joint error S. D. uses 30 df)

D. Bias Prediction: Tectonic-Noise Group Model

Mean:

k \ j	1	2	3	4
1	-0.15	-0.19	-	-
2	0.04	0.05	0.07	-
3	0.20	0.33	0.02	0.03

Error Standard Deviation:

k \ j	1	2	3	4	5
1	0.07	0.02	-	-	-
2	0.10	0.04	0.05	-	-
3	0.11	0.00	0.13	0.01	-
4	-	-	-	-	0.07

(joint error S. D. uses 24 df)

E. Noise Prediction: Tectonic-Noise Group Model

Mean:

k \ j	1	2	3	4
1	0.36	0.71	-	-
2	0.55	0.96	1.35	-
3	0.72	1.12	1.27	1.53

Error Standard Deviation:

k \ j	1	2	3	4	5
1	0.10	0.01	-	-	-
2	0.14	0.15	0.08	-	-
3	0.00	0.00	0.14	0.14	-
4	-	-	-	-	0.12

(joint error S. D. uses 24 df)

TABLE V-1

RELATIONSHIP BETWEEN NOISE LEVEL AND TECTONICS
(PAGE 3 OF 4)

F. Occurrences of Stations in Noise Groups and Tectonic Regions Corrected for Coastline Proximity

33 Stations

k \ j	1	2	3	5
1	5	2	0	7
2	3	6	2	11
3	2	5	8	15
4	10	13	10	33

46 Stations

k \ j	1	2	3	5
1	6	4	0	10
2	5	10	4	19
3	4	5	8	17
4	15	19	12	46

G. Noise Prediction: Line Model Corrected for Coastline Proximity

33 Stations

$\overline{N}_{jk}$:

k \ j	1	2	3
1	0.51	0.89	-
2	0.45	0.92	1.23
3	0.52	0.86	1.20
4	0.49	0.90	1.21

(joint error S. D.=0.08 with 30 df)

46 Stations

$\overline{N}_{jk}$:

k \ j	1	2	3
1	0.50	0.95	-
2	0.51	0.92	1.26
3	0.26	0.86	1.20
4	0.44	0.91	1.22

(joint error S. D.=0.14 with 43 df)

j=1, k=3: (0.36 without coastline correction)
j=1, k=4: (0.48 without coastline correction)

H. Bias and Noise Prediction: Tectonic Model Corrected for Coastline Proximity

33 Stations

Mean:

k	1	2	3
B_k	-0.16	0.06	0.07
N_k	0.46	0.91	1.06

(joint error S. D. for bias=0.10
joint error S. D. for noise=0.24
with 30 df)

46 Stations

Mean:

k	1	2	3
B_k	-0.18	0.12	0.07
N_k	0.50	1.01	0.95

(joint error S. D. for bias=0.11
joint error S. D. for noise=0.33
with 43 df)

TABLE V-1

RELATIONSHIP BETWEEN NOISE LEVEL AND TECTONICS
(PAGE 4 OF 4)

I. Bias Prediction: Tectonic-Noise Group Model Corrected for Coastline Proximity

33 Stations

Mean:

k \ j	1	2	3
1	-0.15	-0.19	-
2	0.04	0.05	0.10
3	0.20	0.10	0.02

(joint error S. D. =0.10 with 25 df)

46 Stations

Mean:

k \ j	1	2	3
1	-0.15	-0.24	-
2	0.11	0.11	0.17
3	0.12	0.10	0.02

(joint error S. D. =0.11 with 38 df)

J. Noise Prediction: Tectonic-Noise Group Model Corrected for Coastline Proximity

33 Stations

Mean:

k \ j	1	2	3
1	0.36	0.71	-
2	0.49	0.97	1.33
3	0.72	0.96	1.21

(joint error S. D. =0.09 with 25 df)

46 Stations

Mean:

k \ j	1	2	3
1	0.35	0.71	-
2	0.62	1.04	1.43
3	0.38	0.96	1.21

(joint error S. D. =0.16 with 38 df)

Part B of Table V-1 shows the noise level of each group (intercept values representing zero bias) for the line model. These levels are determined by averaging observations corresponding to each tectonic classification (shown in row 4) and are very consistent with those obtained for specific tectonic types. The noise levels do not appear to differ significantly between the various tectonic regions. This indicates that the definition of the noise groups is independent of tectonic type. The standard deviations of the noise and bias are computed by taking bias as an independent variable in estimating noise, and likewise taking noise as an independent variable in estimating bias. The fact that the standard deviations of the bias and noise are the same is reflective of the presumed unity of the slope of the straight-line noise-bias relationship. The first four columns of the standard deviation table pertain to the straight-line noise-bias relationship corresponding to each noise group. The fifth column is a combined standard deviation obtained by pooling all four noise groups.

Part C of Table V-1 shows an alternative method, the tectonic model, of statistically estimating the bias and noise. This method is to average the noise and bias observed in each tectonic group. As can be seen in the table, the average noise is different for the various tectonic classifications. The combined standard deviation for bias does not appear to be significantly different from that computed by the noise grouping hypothesis. However, the standard deviations of noise estimated in this manner are considerably higher.

Part D of Table V-1 shows statistical estimates of the bias as mean values corresponding to the tectonic-noise group model. The joint error standard deviation for bias is not significantly different from that obtained from the tectonic model or from the straight-line noise-bias relationship. The joint standard deviation for noise is also approximately the same as that observed in the straight-line model. This observation coupled with the previous observation on the combined standard deviation for noise in the tectonic model

show that classification of the stations by tectonic type alone is not as useful as joint classification by tectonic type and noise group. The bias means of shields (column 3) appears to be significantly lower for high noise and coastal stations. This dichotomy suggests that stations sited in low and medium noise areas on shields should yield far superior detection capability, not only because of lower noise but also because of the larger (more positive) magnitude bias. This suggestion is only based on several low and medium noise stations observed in shield provinces, and should be tested with considerably more data, if possible.

Part E of Table V-1 shows statistical estimates of the noise as mean values corresponding to the tectonic-noise group model. The joint error standard deviation is significantly higher (at a significance level of 0.05) than that obtained from the straight-line noise-bias relationship. The mean noise values for low and medium noise groups (columns 1 and 2) appear to differ significantly and consistently for the three tectonic provinces considered.

Part F of Table V-1 shows the distribution of stations in the noise groups and tectonic provinces after correcting the 33 stations for the incremental noise due to coastline proximity. Similarly corrected noise values are shown for the 46 stations, which include the additional 13 stations.

Part G of Table V-1 shows the group noise values corrected for coastline proximity for the line model. Comparison of part G of Table V-1 for 33 stations to part B of Table V-1, shows that the very high coastal noise group is no longer present, and that the remaining three noise groups are not significantly altered. In the case where 46 stations are evaluated, there is a substantial reduction (0.52 to 0.26) of the average noise level (average $\overline{N}$) for the low noise shield stations (column 1, row 3) from that using 33 stations. This change would have been less, but still probably significant, (0.52 to 0.36) in the absence of the coastline proximity correction for

the 46 station data set. The average noise level for the low noise group for all tectonic provinces (column 1, row 4) changes from 0.49 for the 33 stations values with the coastline proximity correction to 0.44 for the 46 station data set with the coastline proximity correction, which is not considered significant.

Noise and bias values obtained by averaging station noise over each tectonic province are shown in part H of Table V-1. Comparison of the 46 stations and 33 stations is not considered to indicate any significant change.

Part I of Table V-1 gives the mean bias values of the tectonic-noise group model corrected for coastline proximity for the data sets with 33 and 46 stations. In most cases, the means for the data sets are approximately the same.

Part J of Table V-1 shows the corresponding mean noise values of the tectonic-noise group model for the same data sets. As with the mean biases, the majority of the noise means are also approximately the same for the two sets of stations.

As mentioned before, a two-sided t-test was used to compare the noise means for the original 33 stations and the 13 stations with somewhat questionable noise values. The result of this significance test showed that the hypothesis that the two sample means are equal could not be rejected. Therefore, the results obtained when using all 46 stations should be equally valid to those obtained using the 33 stations.

SECTION VI

STATISTICAL HYPOTHESIS TESTS OF MODELS FOR PREDICTING NOISE AND MAGNITUDE BIAS

A one-sided F-test is used to test the models (as tabled in Table V-1) against each other with the goal of determining the best model for predicting magnitude bias and noise. This test allows two sample variances to be compared to determine if one is statistically larger than the other. In this test, the ratio of the variances to be compared results in an F-statistic. In this study, the ratio is determined by dividing the larger variance by the smaller variance. The F-statistic along with the degrees of freedom for the respective variances is then used in conjunction with a table of cumulative F-distributions (Ostle, 1963) to determine whether there is a significant difference between the variances at the significance levels of interest. If the F-statistic is less than the critical F-value for the appropriate significance level, the null hypothesis that the variance in the numerator is less than or equal to the variance in the denominator cannot be rejected. This test was made at 0.01 and 0.05 significance levels. If the null hypothesis has been rejected, the model with the lower variance will be said to be significantly better than the other model.

The various models are compared on the basis of the variance of their noise. Table VI-1 shows the results of these tests. The ranking of the models with respect to increasing noise variance places the line model first, the tectonic-noise group model second, and the tectonic model third. The tests show that the line model is significantly better (99% probability) than a single least-squares representation of all the points, and that the tectonic noise group model and tectonic model are significantly better (99%

TABLE VI-1

SIGNIFICANCE TESTS OF NOISE VARIANCE

Tests	Data Sets			
	33 Observed	33 Corrected	46 Observed	46 Corrected
A	S, 1	S, 1		
B	S, 1	S, 1		
C	S, 2	S, 2		
D	S, 2	N	N	N
E	S, 1	S, 1	S, 1	S, 1
F	S, 1	S, 1	S, 1	S, 1

Tests

A - Test to see if a noise versus bias line model (slope=1.00) for the four observed noise groups or the three corrected noise groups is significantly better than a least squares model assuming only one group.

B - Test to see if the Tectonic-Noise Group model is significantly better than a single noise and bias mean model.

C - Test to see if the Tectonic Model (mean values for each tectonic type) is significantly better than a single noise and bias mean model.

D - Test to see if the line model is significantly better than the Tectonic-Noise Group model.

E - Test to see if the line model is significantly better than the Tectonic model.

F - Test to see if the Tectonic-Noise Group model is significantly better than the Tectonic model.

S - Significant difference

N - No significant difference

1 - Significance level = 0.01 (99% probability)

2 - Significance level = 0.05 (95% probability).

probability) than an overall mean representation. For the 33 station data set with observed noise values, the line model is significantly better than the tectonic-noise group model (95% probability) and over the tectonic model (99% probability). The tectonic-noise group model itself is significantly better than the tectonic model (99% probability). These results show that the line model is clearly the most desirable representation of the bias-noise relationship. The corrected data set shows similar results in that both the line model and tectonic-noise group model are significantly better than the tectonic model (99% probability), and the models are also significantly better than the general representations involving one line or mean (99% probability). However, in this case there is no significant difference between the line and tectonic-noise group models. This lack of any significant difference between the two models is probably due to the shortage of data and some inaccuracies in the noise correction. Since the line model has a smaller noise variance and more degrees of freedom than the tectonic-noise group model, it is still the preferred representation.

As mentioned before, 13 additional stations have been added to the 33 original stations in order to broaden the data base and further test the models. The results of the tests between the models incorporating these additional stations are similar to the results when using the original data base, showing again that the use of these stations is still valid. The line and tectonic-noise group models are significantly better than the tectonic model for both the observed and corrected noise data (99% probability). As before, there is no significant difference between the line and tectonic-noise group models, although the line model is still the preferred interpretation for the same reasons as before.

These tests show that, if possible, the line model should be used to predict the noise. The next best interpretation is the tectonic-noise group model, and the tectonic model is the least preferred representation.

The use of these models to predict bias and noise values will be discussed in a later section.

For completeness, some comments will be made about models for predicting the station magnitude bias. None of the models are significantly better than simply using the mean bias for each tectonic type. The standard deviation of this tectonic model is 0.10 magnitude units; which compares with 0.08 for the line model. However, the line model required a priori knowledge of the noise group and the noise level, while the tectonic model only requires knowledge of the tectonic type.

SECTION VII
METHODOLOGY OF NETWORK CAPABILITY EVALUATION

The computer program NETPROB is used to estimate the capability of a network consisting of 100 stations. NETPROB is a modified version of another program called NET2 (Snell, 1976), which is itself based on a program called NETWORTH (Wirth, 1970). Instead of determining the magnitude detection threshold for a given probability of detection as is done in NET2 and NETWORTH, the network probability is determined for a given magnitude. The technique in NET2 for estimating network detection capability is based on the equations in Table VII-1 (Snell, 1976). First, the signal amplitudes at all network stations are calculated for an assumed event at epicenter j with a given magnitude m_{b_j} (equation (VII-1)). The calculation of the signal amplitudes uses a standard distance-amplitude table based upon Clawson P-wave values (Clawson and Veith, 1972). Signal and noise are assumed lognormally distributed in NET2; hence the probability that the signal-to-noise ratio exceeds the station detection threshold is given by the normal cumulative probability function (equations (VII-2) and (VII-3)). In NET2, the signal and noise are recorded as zero-to-peak (0-p) amplitudes. The noise mean is input as the geometric mean of the noise amplitude; the logarithm of the geometric mean gives the mean logarithm (base 10) of the noise, μ_N. The individual station detection probabilities are then combined into a network probability of at least α station detections, $p_j(\geq \alpha)$, using a recursive relation involving the individual station probabilities (equation (VII-4)). The network detection probabilities determined in this study represent the probability of at least 4 stations detecting (i.e., $\alpha = 4$).

TABLE VII-1

EVALUATION OF NETWORK DETECTION CAPABILITY

$$\log_{10} A_{ij} = m_j + b_\Delta + c_\Delta \log_{10} \Delta_{ij} + E_{ij} \qquad \text{(VII-1)}$$

$$p_{ij} = \phi \left[\frac{\log_{10} A_{ij} - (\mu_N + \log_{10} SDT)}{\sigma_r^2 + \sigma_s^2)^{1/2}} \right] \qquad \text{(VII-2)}$$

$$\phi(x) = \frac{1}{\sqrt{2\pi}} \int_{\infty}^{x} e^{-y^2/2} \, dy \qquad \text{(VII-3)}$$

$$\hat{p}_j(\geq \alpha) = \sum_{k=\alpha}^{N} \hat{p}_j(k) \qquad \text{(VII-4)}$$

Symbols above are defined as follows:

- A_{ij} - signal amplitude at station i for event j (0-p)
- m_j - magnitude of event j (m_b)
- b_Δ, c_Δ - standard table entries
- E_{ij} - station-epicenter bias correction
- μ_N - mean $\log_{10}$ noise amplitude (0-p)
- σ_n^2 - variance of $\log_{10}$ noise
- σ_n^2 - variance of $\log_{10}$ signal
- $\phi(x)$ - normal cumulative probability function
- N - number of stations in the network
- $\hat{p}_j(k)$ - probability that k stations will detect event j
- $\hat{p}_j(\geq \alpha)$ - probability that α or more stations will detect event j
- SDT - station detection threshold, i.e., signal-to-noise ratio required for detection at station.

The calculation of confidence regions is based upon the estimated travel-time variance, which has an individual station component and a station-epicenter component derived from a standard table (Herrin, 1968). In the present study, 0.30 seconds was used as the standard deviation of the travel-time. This value was obtained by Unger (1977) in designing an automatic P-wave timing algorithm. The confidence regions are elliptical since the derivations of the travel-time variance with respect to latitude and with respect to longitude are in general not equal, varying with the epicenter/network configuration. The confidence regions are centered upon the known epicenters (Snell, 1976). An event, occurring at each epicenter with magnitude equal to the network threshold magnitude, will be located within the error ellipse calculated for the given location probability (95% in the present study).

Several modifications have been made to the original NETPROB program, see Table VII-2. The most significant of the changes is the expansion of the maximum network size to 100 stations. This change involves the necessity of distilling the stations down to a total of less than 27 probability value in order to alleviate truncation error in the probability calculation (Wirth, 1970).

A grouping test is applied to ordered detection probabilities in order to determine if several probability values can be represented as one value within a given error. The test is applied as an iterative procedure starting with one probability value and adding more until either a desired maximum number of values is reached or the test is failed. The grouping test is illustrated by equation (VII-5):

$$\underbrace{\left(1 - \prod_{i=1}^{N} q_i\right)}_{\substack{P_D \text{ for at} \\ \text{least one} \\ \text{station}}} - \underbrace{\left(\prod_{i=1}^{N} q_i\right) \sum_{i=1}^{N} \frac{p_i}{q_i}}_{\substack{P_D \text{ for exactly} \\ \text{one station}}} < X \qquad \text{(VII-5)}$$

TABLE VII-2

NETPROB MODIFICATIONS

- Outputs epicenter tables (includes P_D, azimuth, and distance for each station)
- Computes error ellipses weighted by P_D for each station
- Computes P_D for error ellipse of 10,000 km^2
- Computes average bias of network from the station corrections weighted by corresponding P_D
- Network capacity increased to 100 stations
- Option for including signal standard deviations for each station
- Option to set P_D to zero for epicentral distances $<\Delta_o$
- Option to correct the station detection probability for a mixed event
- Contour the exponent of the ratio of successes to failures, $\log_{10} (P_D/1-P_D)$
- Contour network magnitude bias
- Contour location error ellipse areas
- Contour $\log_{10}(P_D/1-P_D)$ for probability of location within a 10,000 km^2 error ellipse.

where p is the probability of detection (also represented as P_D) of a given event; q is the probability of not detecting the event; N is the number of values; and X is some arbitrary number set to group the station detection probability values as desired. A maximum number of stations per group is also set. In the present study, X has a value of 0.1225, and the maximum number of stations per group is ten. This value of X combines the stations into less than 27 probability values for most of the epicenters. The test limit, X, was determined by trial-and-error testing of the station grouping method.

In the present application of this test, a value of 0.1225 for X makes it impossible to represent two 0.35 probability values as a single probability. In other words, for probability values less than 0.35, it is possible to represent several probability values as a single value with an error of at most 0.1225. Higher values of X result in greater concentration of station probabilities into groups because higher probabilities can be grouped. Although, this grouping lowers the truncation error, the grouping error associated with representing several probabilities as one increases. Lower values of X result in less grouping of stations (i.e., more individual probabilities), because the probability range that can be grouped is smaller. The corresponding truncation and grouping errors are larger and smaller, respectively. Limiting the maximum number of values per group affects the total number of resultant groups and thereby the truncation error. It also tends to limit the grouping error within each group by finishing off a group before the maximum error is reached. The choice of an X value therefore involves a trade-off between truncation error and grouping error.

In practice, the detection probabilities, P_D's, are first calculated for each station and the probabilities are then ordered from highest to lowest. The values are then tested for grouping starting with the lowest value. Station probabilities are combined as long as the difference between the probability value for the group and the probability value for exactly one station is

less than the set value, X, and N does not exceed the maximum number of stations per group. The probability of detection for the group is taken as $(1 - \prod_{i=1}^{N} q_i)$, the left term of equation (VII-5). Station grouping is only used in the network probability calculations.

The other modifications are added mainly to make the program more realistic. The change to error ellipse calculations simply involves multiplying the P_D for each station times the respective parameters involved in the location calculations. The sum of the station detection probabilities, P_D, is the expected number of stations detecting the hypothetical event. An option to zero out the station P_D for stations within a given distance from the epicenter is included; however, this capability is not used in the present network study. In addition, the network probability of location within a 10,000 km^2 area is calculated from values determined in the regular error ellipse calculations. The average network magnitude bias for a given event is calculated from the station corrections, representing individual station magnitude biases, weighted by the P_D of each station for an event of the given magnitude at each epicenter. The correction for the probability of a mixed event is applied by making the station probability of detection, P_D, a conditional probability involving not only the ideal P_D and the probability the station is working, but also the probability that the event is not mixed. The rest of the modifications listed involve the output from the program.

SECTION VIII

APPLICATION OF NOISE AND BIAS MODELS TO NETWORK CAPABILITY ESTIMATION

The station parameters and models discussed in the preceding sections are used in evaluating the detection capability of a network of 100 stations. As seen in Figure VIII-1A, the noise groups for the 46 station data set incorporating noise amplitudes corrected for ocean noise are fairly consistent over significant geographical areas. Comparison of Figures VIII-1A and VIII-1B shows that the noise groups are also correlated with tectonic structure to some extent.

A scheme for assigning either bias or noise values can be developed after making this observation. It is assumed that the tectonic structure of the receiver site can always be determined from a tectonic map. The noise group can be determined for areas in the vicinity of the stations used in this study by using the noise group of the nearest station. If both the bias and noise values are known, as is the case with the stations used to determine the various models, these parameters will be used. If only the group, bias, and tectonic type are known, the noise value will be obtained from the line model. However, if the group, noise, and tectonic type are known, the bias will be determined from the tectonic-noise group model. Finally, if the noise group is not known the tectonic model will be used to obtain the unknown terms. In all the above cases, the model with the smallest variance from which the unknown terms can be determined is used.

A standard deviation of 0.34 magnitude units was determined to be the average signal standard deviation, σ_{signal}, based on values given by North (1977). The average standard deviation of the noise is assumed to be

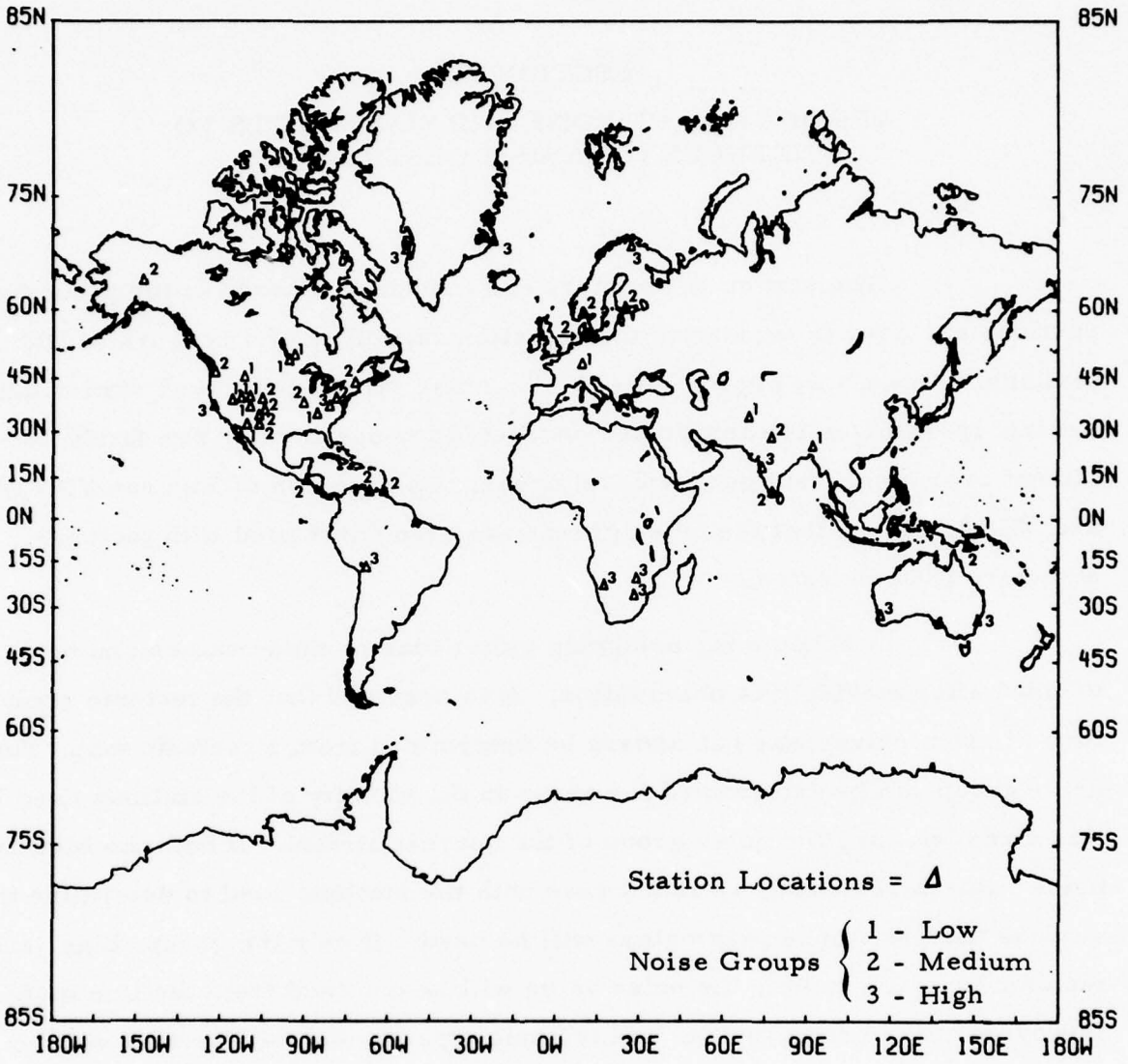

FIGURE VIII-1A

GEOGRAPHIC DISTRIBUTION OF NOISE GROUPS

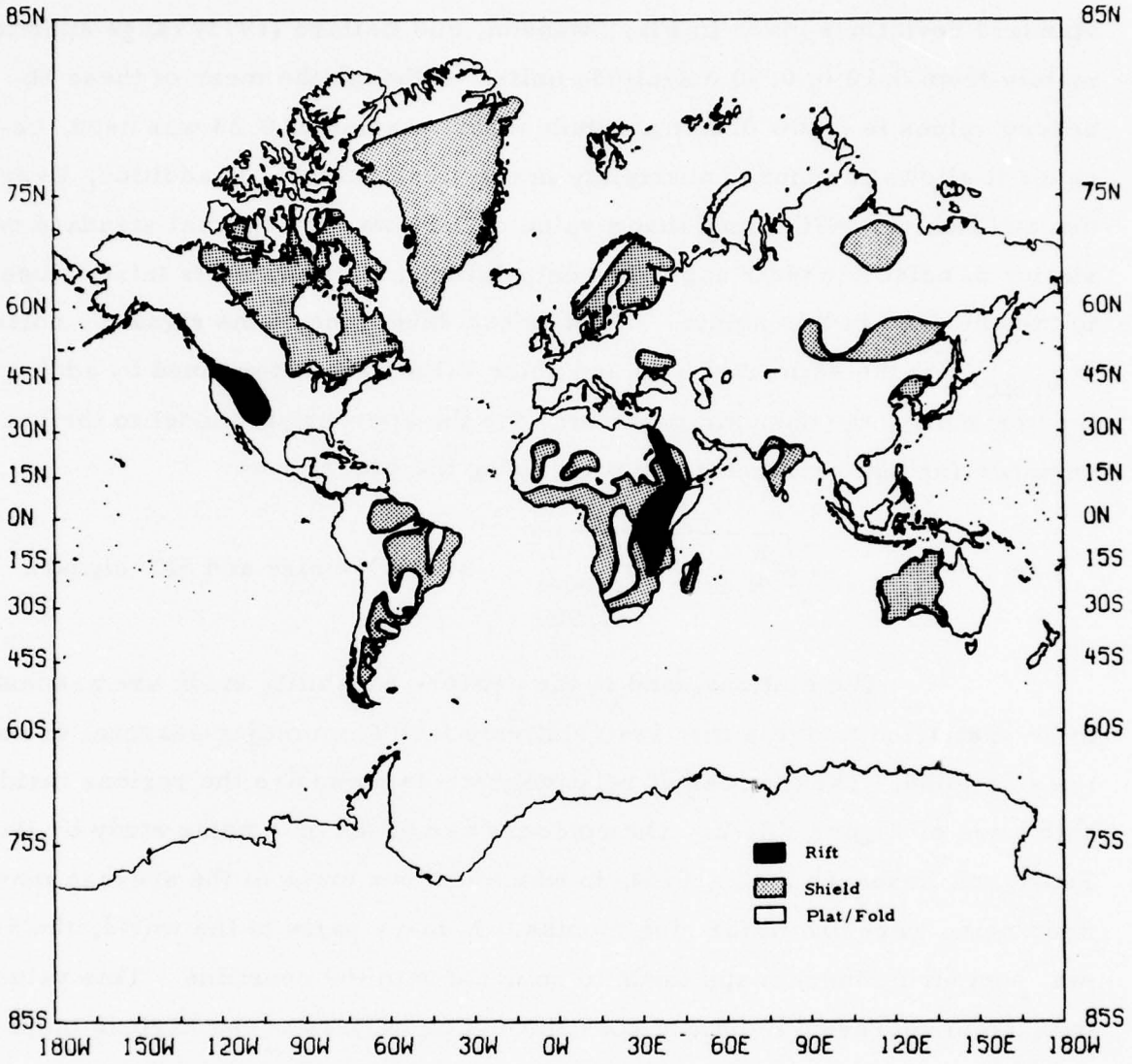

FIGURE VIII-1B

WORLD-WIDE TECTONIC STRUCTURE
(MODIFIED FROM SMITH (1973) AND KUMMEL (1970))

0.23 magnitude units since observed values are on this order. The observed standard deviations given in Fix, Swanson, and Ballard (1973) range approximately from 0.10 to 0.30 magnitude units. Although the mean of these observed values is below 0.20 magnitude units, a value of 0.23 was used, because it allows for more uncertainty in the noise values. In addition, Evernden and Kohler (1976) found that a value of 0.21 was the optimal standard deviation of noise for their capability calculations. This value is fairly close to the one used in this study. The standard deviations of the signal or noise, $\sigma_{N,SIG}$, for the estimated bias and noise values are determined by adding the variance of the unknown parameter for the appropriate model to the base variance for that parameter and then taking the square root:

$$\text{(i.e., } \sigma_{N,SIG} = \sqrt{\sigma^2_{N,SIG} + \sigma^2_{\substack{\text{Model} \\ N,SIG}}} \text{, where N=noise and SIG=signal).}$$

The stations used in the network capability study are assumed to be restricted to areas that are relatively free from major seasonal variations in noise. These areas of relatively stable noise are the regions inside both lines of Figure VIII-2. The contours are based on a noise study by Hair, Funk, and Research Staff (1964), in which contour maps of the average maximum noise were drawn for nine months. In many parts of the world, the 50 $m\mu$ contour on these maps tends to coincide with the coastline. This value is taken to represent the noise coastline. Comparison of the various maps shows that the noise coastline fluctuates in places according to the season, winter being noisier in general than summer. The contours in Figure VIII-2 represent the approximate position of the noise coastline for these seasons. The boundaries of the relatively stable areas follow the coastline in general, but in some regions, they cut across continental boundaries. The exact reason for this is not known. One, however, can conjecture that the cutting of seasonal ocean noise boundaries across continental areas, such as the eastern United States and Canada, appears sometimes to be associated with

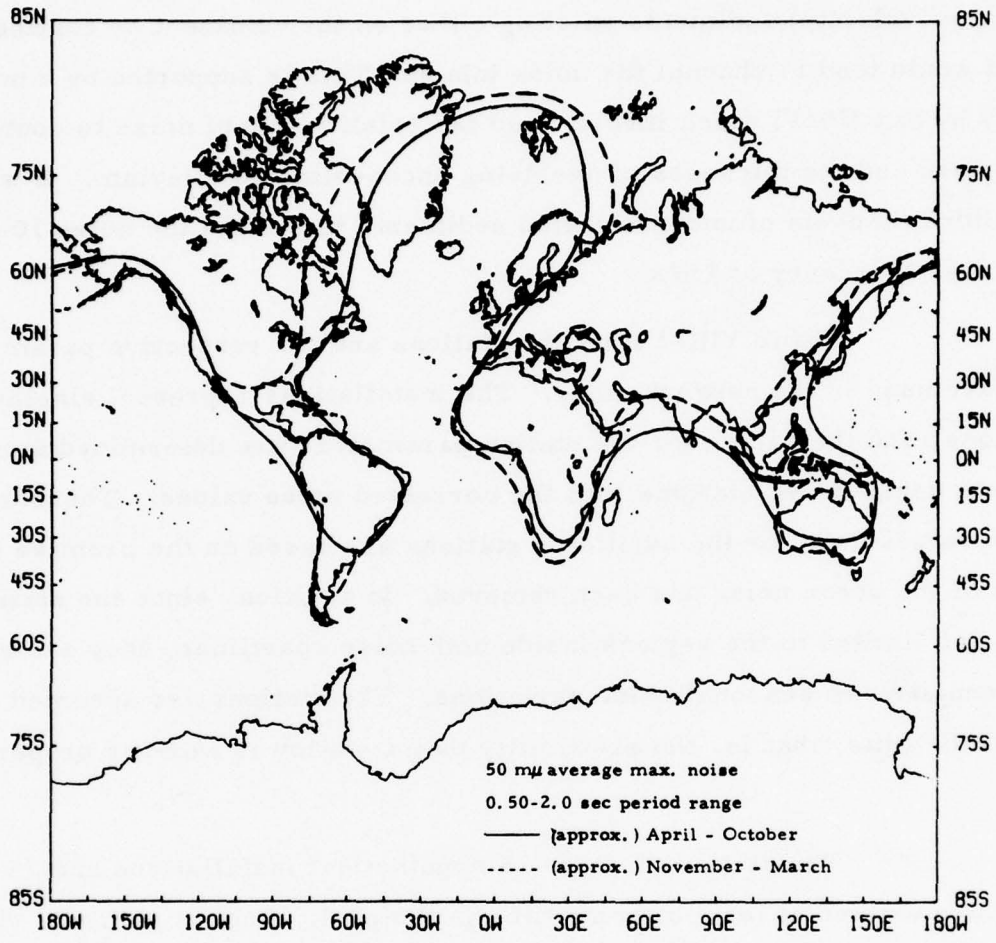

FIGURE VIII-2

SEASONAL EXTREMES OF 50 mμ NOISE CONTOUR

transgressive ocean shorelines. In that case, recent sedimentary wedges of soft (low velocity) sediments existing either on the continent or continental shelf would tend to channel the noise inland. This is supported by a noise study by Sax (1965) which investigated the relationship of noise to continental structure and the thickness of overlying unconsolidated alluvium. It was found that thick blankets of unconsolidated sediments increased the noise 10-20 dB at a peak frequency of 1 Hz.

Table VIII-1 lists the stations and the respective parameters that are used in the network study. The installations represent single-site stations, and the values for the station parameters are determined from the models using the 46 stations with the corrected noise values. Therefore, the noise values used for the additional stations are based on the premise that most of the ocean noise has been removed. In addition, since the stations used are limited to the regions inside both noise coastlines, they are relatively insensitive to seasonal noise variations. The stations are assumed to be up all the time, that is, the probability that a station is working properly is one.

The stations include 25 hypothetical installations and 75 stations that have existed at least at some time in the past, if not at present. The locations of the stations do not take political, environmental, or geographical boundaries into account.

The detection capability of two networks is studied for an event m_b of 4.0. The probability of a mixed event is assumed to be zero. The negative of the bias values for each station is applied as a station correction in order to reduce network bias due to receiver region anomalies. A 4.0 m_b figure is used because it is the lowest m_b for which the bias corrections are effective in reducing scatter (North, 1977).

TABLE VIII-1

STATIONS USED IN NETWORK EVALUATION
(PAGE 1 OF 5)

Noise values are given in Log_{10}(peak-to-peak) (p-p).

Source Key for Station Lists

A	North (1977)
B	Everinden and Kohler (1976)
C	The Geotechnical Corporation (1965)
D	Fix, Swanson, and Ballard (1973)
E	Hair, Funk, and Research Staff (1964)
F	Line Model
G	Tectonic-Noise Group Model
H	Tectonic Model
I	National Earthquake Information Center (1970)
J	The Geotechnical Corporation (1964)
K	Approximate
L	Personal communication, Chang, A.C.
M	Strauss (1976)

Tectonic Types

R	Rift zone; or region with similar upper mantle structure
P/F	Platform and fold belts
S	Shield
*	Hypothetical stations

Noise Groups:

1	Low
2	Medium
3	High
4	Very High (coastal)

TABLE VIII-1

STATIONS USED IN NETWORK EVALUATION
(PAGE 2 OF 5)

Name	Latitude	Longitude	Tectonic Type	Grouping for Corrected Noise	Bias	Observed Noise	Corrected or Estimated Noise	(0-p) Noise	σ_{signal}	σ_{noise}	Source		
											Bias	Noise	Location
BMO	44.849 N	117.306 W	R	2	-0.29		0.622	2.094	0.34	0.26	A	F	I
NEW	48.263 N	117.120 W	R	2	0.05		0.962	4.581	0.34	0.26	A	F	I
TFO	34.268 N	111.270 W	R	1	-0.32		0.119	0.658	0.34	0.26	A	F	I
LAO	46.689 N	106.222 W	P/F	2	-0.10		0.812	3.243	0.34	0.26	A	F	I
RCD	44.075 N	103.208 W	P/F	2	-0.24		0.672	2.349	0.34	0.26	A	F	I
WMO	34.718 N	98.589 W	P/F	2	-0.17		0.742	2.760	0.34	0.26	A	F	I
TUL	35.911 N	95.589 W	P/F	2	0.21		1.122	6.622	0.34	0.26	A	F	I
ROL	37.918 N	91.869 W	P/F	2	0.20		1.112	6.471	0.34	0.26	A	F	I
ATL	33.433 N	84.338 W	P/F	2	0.35		1.262	9.141	0.34	0.26	A	F	I
GIL	64.975 N	147.495 W	P/F	2	-0.04		0.872	3.724	0.34	0.26	A	F	I
INK	68.292 N	133.500 W	S	1	0.15		0.589	1.941	0.34	0.26	A	F	I
PNT	49.317 N	119.617 W	P/F	2	0.13		1.042	5.508	0.34	0.26	A	F	I
EDM	53.222 N	113.350 W	P/F	2	0.37		1.282	9.571	0.34	0.26	A	F	I
FFC	54.725 N	101.978 W	S	1	0.08		0.519	1.652	0.34	0.26	A	F	I
CMC	67.833 N	115.083 W	S	1	0.12	1.041	0.699	2.333	0.36	0.23	G	D	I
ILG	77.947 N	39.183 W	S	2	0.04		0.952	4.477	0.34	0.26	A	F	I
CLL	51.309 N	13.004 E	P/F	1	0.20		0.639	2.178	0.34	0.26	A	F	I
GRF	49.692 N	11.215 E	P/F	1	0.24		0.679	2.388	0.34	0.26	A	F	I
BRG	50.874 N	13.946 E	P/F	1	-0.11		0.329	1.067	0.34	0.26	A	F	I
MOX	50.646 N	11.616 E	P/F	1	0.02		0.459	1.439	0.34	0.26	A	F	I
BUH	48.675 N	8.228 E	P/F	1	0.04		0.479	1.507	0.34	0.26	A	F	I
PRU	49.988 N	14.542 E	P/F	1	0.04		0.479	1.507	0.34	0.26	A	F	I
KHC	49.131 N	13.579 E	P/F	1	0.10		0.539	1.730	0.34	0.26	A	F	I
FUR	48.166 N	11.271 E	P/F	1	0.10		0.539	1.730	0.34	0.26	A	F	I
LJU	46.043 N	14.533 E	P/F	1	0.29		0.729	2.679	0.34	0.26	A	F	I

TABLE VIII-1

STATIONS USED IN NETWORK EVALUATION
(PAGE 3 OF 5)

Name	Latitude	Longtitude	Tectonic Type	Grouping for Corrected Noise	Bias	Observed Noise	Corrected or Estimated Noise	(0-p) Noise	σ_{signal}	σ_{noise}	Source		
											Bias	Noise	Location
ANT	23.705S	70.415W	P/F	3	0.17	1.586	1.214	8.184	0.36	0.23	G	D	I
PNS	16.267S	68.473W	P/F	3	-0.08		1.139	6.886	0.34	0.26	A	F	I
*BRZ1	6.000S	53.000W	S	-	0.07		0.945	4.405	0.36	0.40	H	H	K
*BRZ2	17.000S	53.000W	P/F	-	0.12		1.008	5.093	0.36	0.40	H	H	K
*XXQ	11.000S	43.000W	S	-	0.07		0.945	4.405	0.36	0.40	H	H	K
*MOS	55.500N	38.000E	P/F	1	0.11		0.616	2.065	0.36	0.28	G	G	K
*TUR	64.000N	100.000E	P/F	-	0.12		1.008	5.093	0.36	0.40	H	H	K
*ZYR	65.500N	151.000E	P/F	-	0.12		1.008	5.093	0.36	0.40	H	H	K
*ZAY	47.500N	85.500E	P/F	1	0.11		0.616	2.065	0.36	0.28	G	G	K
*TOB	58.000N	68.000E	P/F	-	0.12		1.008	5.093	0.36	0.40	H	H	K
*YAK	62.000N	129.000E	P/F	-	0.12		1.008	5.093	0.36	0.40	H	H	K
*VOL	71.500N	94.500E	P/F	-	0.12		1.008	5.093	0.36	0.40	H	H	K
*CHK	29.000N	106.500E	P/F	-	0.12		1.008	5.093	0.36	0.40	H	H	K
*TSI	47.000N	124.000E	P/F	-	0.12		1.008	5.093	0.36	0.40	H	H	K
*ULB	48.000N	107.000E	P/F	-	0.12		1.008	5.093	0.36	0.40	H	H	K
*TAY	37.800N	112.800E	P/F	-	0.12		1.008	5.093	0.36	0.40	H	H	K
*YUSH	37.800N	91.000E	P/F	1	0.11		0.616	2.065	0.36	0.28	G	G	K
BXUT	37.563N	109.435W	R	1	-0.18	0.43	0.43	1.35	0.34	0.23	B	B	L
LCNM	32.402N	106.599W	R	2	-0.17	0.70	0.70	2.56	0.34	0.23	B	B	J
EUR	39.483N	115.970W	R	1	-0.24	0.40	0.40	1.26	0.34	0.23	A	B	I
DUG	40.195N	112.813W	R	1	-0.15	0.398	0.398	1.250	0.34	0.23	A	B	I
BOZ	45.600N	111.633W	R	1	-0.06	0.398	0.398	1.250	0.34	0.23	A	B	I
UBO	40.322N	109.569W	R	1	-0.11	0.176	0.176	0.750	0.34	0.23	A	B	I
ALQ	34.942N	106.459W	R	2	-0.20	0.710	0.710	2.564	0.34	0.23	A	B	I
GOL	39.700N	105.371W	R	2	-0.28	0.699	0.699	2.500	0.34	0.23	A	E	I
LON	46.750N	121.810W	R	2	-0.30	0.954	0.742	2.760	0.34	0.23	A	E	I
TUC	32.310N	110.782W	R	1	-0.14	0.477	0.317	1.037	0.34	0.23	A	E	I

TABLE VIII-1

STATIONS USED IN NETWORK EVALUATION
(PAGE 4 OF 5)

Name	Latitude	Longitude	Tectonic Type	Grouping for Corrected Noise	Bias	Observed Noise	Corrected or Estimated Noise	(0-p) Noise	σ_{signal}	σ_{noise}	Source		
											Bias	Noise	Location
KRA	50.056 N	19.940 E	P/F	1	0.22		0.659	2.280	0.34	0.26	A	F	I
NIE	49.424 N	20.322 E	P/F	1	-0.02		0.419	1.312	0.34	0.26	A	F	I
TOL	39.881 N	4.049 W	P/F	-	0.12	1.571	1.411	12.882	0.36	0.23	H	D	I
*POL	52.000 N	21.000 E	P/F	1	0.11		0.616	2.065	0.36	0.28	G	G	K
BHA	14.447 S	28.468 E	R	-	-0.28		0.497	1.570	0.34	0.40	A	H	I
MTD	16.750 S	31.500 E	R	-	-0.22		0.497	1.570	0.34	0.40	A	H	K
KRR	16.852 S	29.618 E	R	-	-0.24		0.497	1.570	0.34	0.40	A	H	I
CIR	21.013 S	31.580 E	R	-	-0.27		0.497	1.570	0.34	0.40	A	H	I
CLK	15.680 S	34.977 E	R	-	-0.27		0.497	1.570	0.34	0.40	A	H	I
BNG	4.367 N	18.567 E	R	-	-0.07		1.008	5.093	0.34	0.40	A	H	I
*AAE2	9.029 N	38.766 E	R	-	-0.18		0.497	1.570	0.36	0.40	H	H	I
*KEN	1.500 N	35.000 E	R	-	-0.18		0.497	1.570	0.36	0.40	H	H	K
*MAL	19.000 N	2.000 E	P/F	-	0.12		1.008	5.093	0.36	0.40	H	H	K
*CHD	16.000 N	16.000 E	P/F	-	0.12		1.008	5.093	0.36	0.40	H	H	K
*ALG	30.000 N	3.000 E	P/F	-	0.12		1.008	5.093	0.36	0.40	H	H	K
EIL	29.550 N	34.950 E	R	-	-0.18	0.845	0.473	1.486	0.36	0.23	H	D	I
SHI	29.638 N	52.520 E	P/F	1	0.11	1.111	0.739	2.741	0.36	0.23	G	D	I
MSH	36.311 N	59.588 E	P/F	1	0.11	0.812	0.812	3.240	0.36	0.23	G	M	I
QUE	30.188 N	66.950 E	P/F	1	0.11	0.706	0.706	2.541	0.36	0.23	G	D	I
NIL	33.650 N	73.252 E	P/F	1	0.11	0.894	0.894	3.917	0.36	0.23	G	D	I
ASP	23.500 S	133.600 E	S	-	-0.05		0.945	4.405	0.34	0.40	A	H	K
CTA	20.088 S	146.254 E	P/F	-	0.12	1.274	0.995	4.943	0.36	0.23	H	D	I
*TRKY	17.000 S	128.000 E	S	-	0.07		0.945	4.405	0.36	0.40	H	H	K
*NULL	22.000 S	120.100 E	S	-	0.07		0.945	4.405	0.36	0.40	H	H	K
*BULG	26.500 S	143.800 E	P/F	-	0.12		1.008	5.093	0.36	0.40	H	H	K
*BOR	16.250 S	137.000 E	S	-	0.07		0.945	4.405	0.36	0.40	H	H	K
CHG	18.790 N	98.977 E	P/F	-	0.12	0.861	0.649	2.228	0.36	0.23	H	D	I
BOG	4.623 N	74.065 W	P/F	3	0.17	1.920	1.837	34.353	0.36	0.23	G	D	I

TABLE VIII-1

STATIONS USED IN NETWORK EVALUATION
(PAGE 5 OF 5)

Name	Latitude	Longitude	Tectonic Type	Grouping for Corrected Noise	Bias	Observed Noise	Corrected or Estimated Noise	(0-p) Noise	σ_{signal}	σ_{noise}	Source		
											Bias	Noise	Location
CPO	35.595 N	85.570 W	P/F	1	-0.07	0.398	0.398	1.250	0.34	0.23	A	B	I
KBL	34.541 N	69.043 E	P/F	1	0.09	0.562	0.562	1.824	0.34	0.23	A	D	I
SHL	25.567 N	91.883 E	P/F	1	0.11	0.683	0.523	1.667	0.34	0.23	A	D	I
STU	48.771 N	9.193 E	P/F	1	0.29	0.845	0.793	3.104	0.34	0.23	A	E	I
COL	64.900 N	147.793 W	P/F	2	0.01	0.990	0.938	4.335	0.34	0.23	A	D	I
FLO	38.802 N	90.370 W	P/F	2	0.26	1.255	1.255	8.994	0.34	0.23	A	E	I
CAR	10.507 N	66.928 W	P/F	2	0.13	1.342	0.970	4.666	0.34	0.23	A	E	I
TRN	10.649 N	61.403 W	P/F	2	0.07	1.491	1.119	6.576	0.34	0.23	A	E	I
RTNM	36.729 N	104.361 W	P/F	2	0.09	0.90	0.90	3.97	0.34	0.23	B	B	J
PMG	9.409 S	147.154 E	P/F	2	0.10	1.366	0.994	4.931	0.34	0.23	A	D	I
LPB	16.533 S	68.098 W	P/F	3	0.07	1.318	1.203	7.979	0.34	0.23	A	D	I
EBMT	49.628 N	95.622 W	S	1	0.12	0.716	0.716	2.600	0.34	0.23	B	C	L
RKON	50.839 N	93.672 W	S	1	0.28	0.716	0.716	0.716	0.34	0.23	B	C	J
RES	74.687 N	94.900 W	S	1	0.13	0.000	0.000	0.500	0.34	0.23	A	E	I
ALE	82.483 N	62.400 W	S	1	-0.04	0.477	0.105	0.637	0.34	0.23	A	E	I
NDI	28.683 N	77.217 E	S	2	0.33	1.109	1.109	6.426	0.34	0.23	A	D	I
NOR	81.600 N	16.683 W	S	2	-0.14	1.102	0.730	2.685	0.34	0.23	A	D	I
WIN	22.567 S	17.100 E	S	3	-0.09	1.331	1.119	6.576	0.34	0.23	A	D	I
PRE	25.753 S	28.190 E	S	3	-0.07	1.331	1.279	9.505	0.34	0.23	A	D	I
BUL	20.143 S	28.613 E	S	3	-0.07	1.134	1.134	6.807	0.34	0.23	A	D	I

The first network consists of the 100 single-site stations listed in Table VIII-1 and the second network consists of 72 single-site stations and 28 simulated arrays. The arrays, Table VIII-2, are located in the lower latitudes and around the Pacific Ocean. These regions have been chosen because they are the weakest areas of detection for the first network, and substitution of arrays for some of the stations in these areas will increase the detection capability of the network. Figure VIII-3 shows the geographic distribution of the station locations in the networks. The 28 arrays are simulated by choosing the single-site stations with the lowest noise, most positive bias, and desired location and then dividing the noise amplitude ($m\mu$, p-p) by four. This results in a noise value which is reasonable for a 19-element array at the site of the single-site station and allows a signal loss of 0.75 dB. A signal-to-noise ratio of 3.00 is assumed necessary for detection of a short-period signal by stations in either network. This ratio corresponds to an automatic detector false alarm rate of 5 false alarms per hour (Swindell and Snell, 1977).

Figure VIII-4 shows global contours of the Fisher transformation of network detection probabilities (at least 4 stations detection), $\log_{10}(P_D/(1-P_D))$, which measures the exponent of successes to failures (contour interval = 1) for the network consisting of 100 single-site stations. The contours on this and following figures are based on 275 points (epicenters) between 75°N, S and 180°E, W with a 15° spacing between points. Table VIII-3 is a conversion table between the value for the Fisher transformation and the network probability of detection. As can be seen in Figure VIII-4, the probability of at least 4 stations detection a 4.0 m_b event for the 100 single-site stations is greater than 50% (0 contour) for most of the world, except in parts of the southern hemisphere.

Figure VIII-5 shows global contours of the 95% confidence error ellipse areas in 5,000 km^2 intervals for the same network. An upper

TABLE VIII-2

LOWER LATITUDE CIRCUM-PACIFIC SIMULATED ARRAYS
(Array Noise Values = Single Site Noise Amplitude/4)

Name	Noise (0-p)mμ
South America	
ANT	2.046
BRZZ	1.273
XXQ	1.101
CAR	1.167
LPB	1.995
Australia	
ASP	1.101
CTA	1.236
TRKY	1.101
BULG	1.273
BOR	1.101
Africa	
BNG	1.273
AAEZ	0.393
BUL	1.702
PRE	2.376
CHD	1.273
South East Asia and China	
CHG	0.557
CHK	1.273
TAY	1.273
TSI	1.273
ULB	1.273
USSR	
ZYR	1.273
YAK	1.273
Western U.S. and Canada	
COL	1.084
PNT	1.377
BOZ	0.313
NEW	1.145
UBO	0.188
TUL	0.259

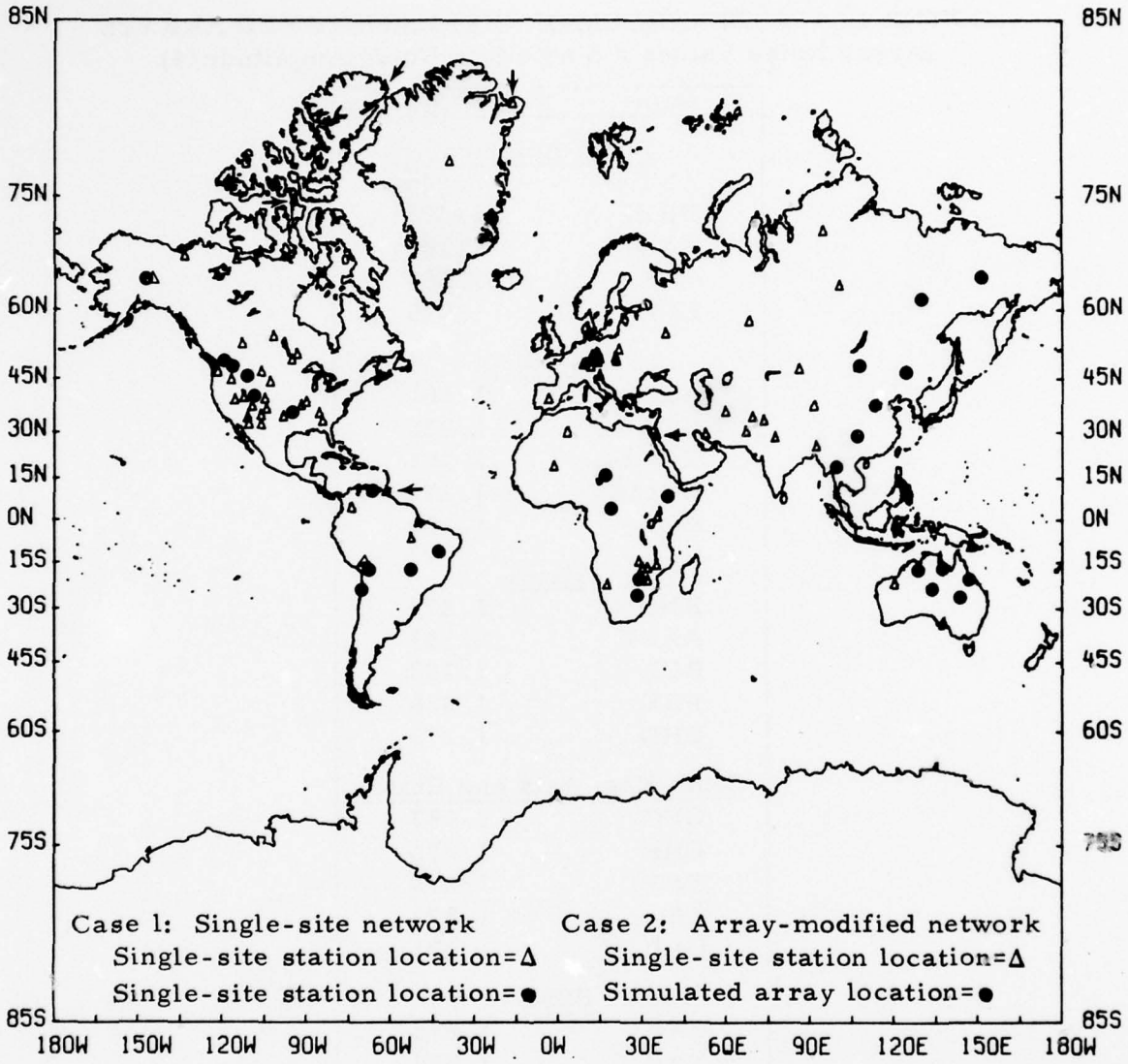

FIGURE VIII-3

GEOGRAPHIC DISTRIBUTION OF NETWORK RECEIVERS

TABLE VIII-3

CONVERSION TABLE FOR PROBABILITY OF DETECTION, P_D, CONTOURS

$\text{Log}(\frac{P_D}{1-P_D})$	P_D
5.0	0.99999
4.0	0.99900
3.0	0.99900
2.0	0.99010
1.0	0.90909
0.0	0.50000
-1.0	0.09090
-2.0	0.00990
-3.0	0.00100
-4.0	0.00010
-5.0	0.00001

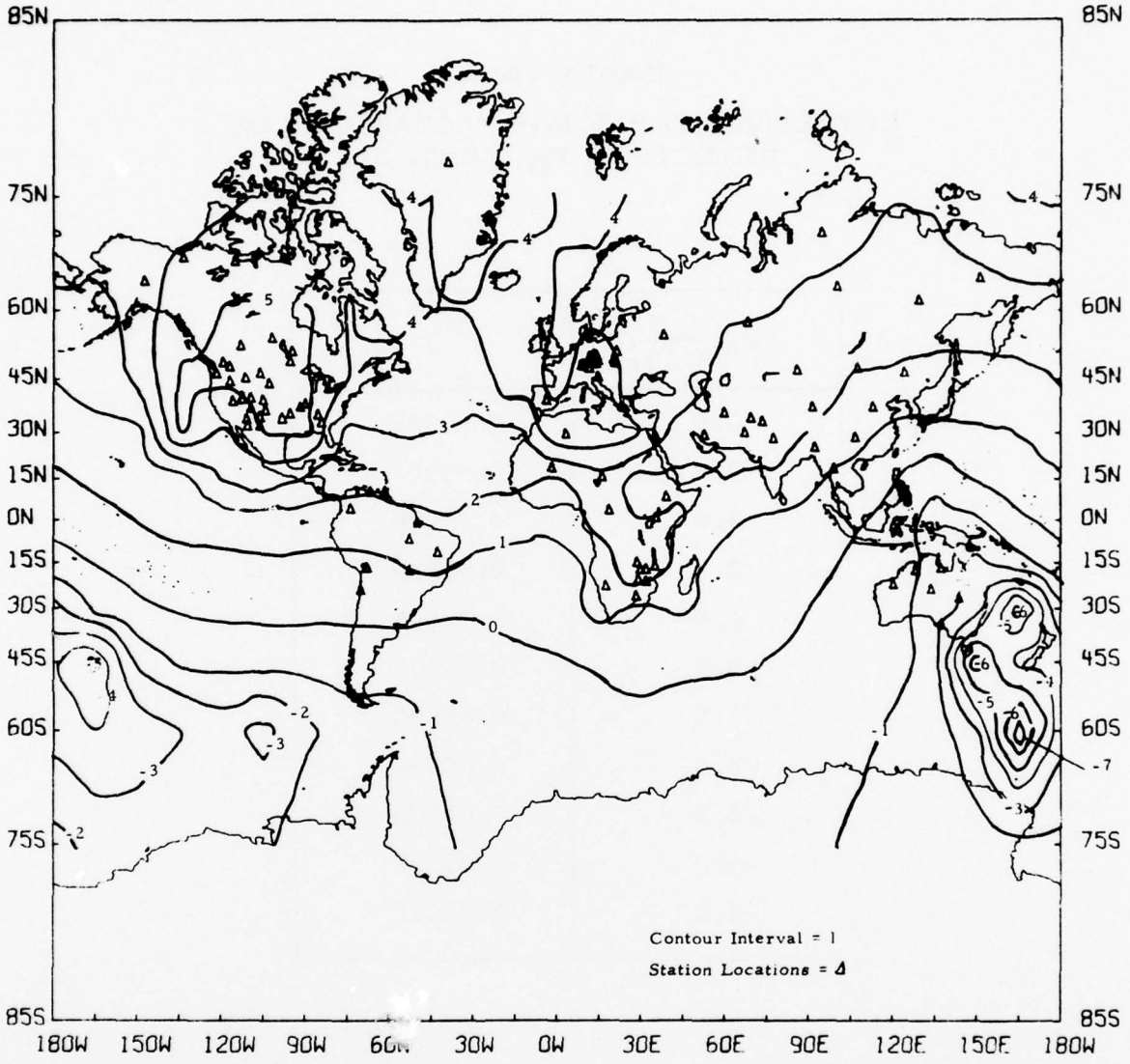

FIGURE VIII-4

LOG ($P_D/(1-P_D)$) OF DETECTION PROBABILITY FOR 100 STATION NETWORK
(m_b = 4.0)

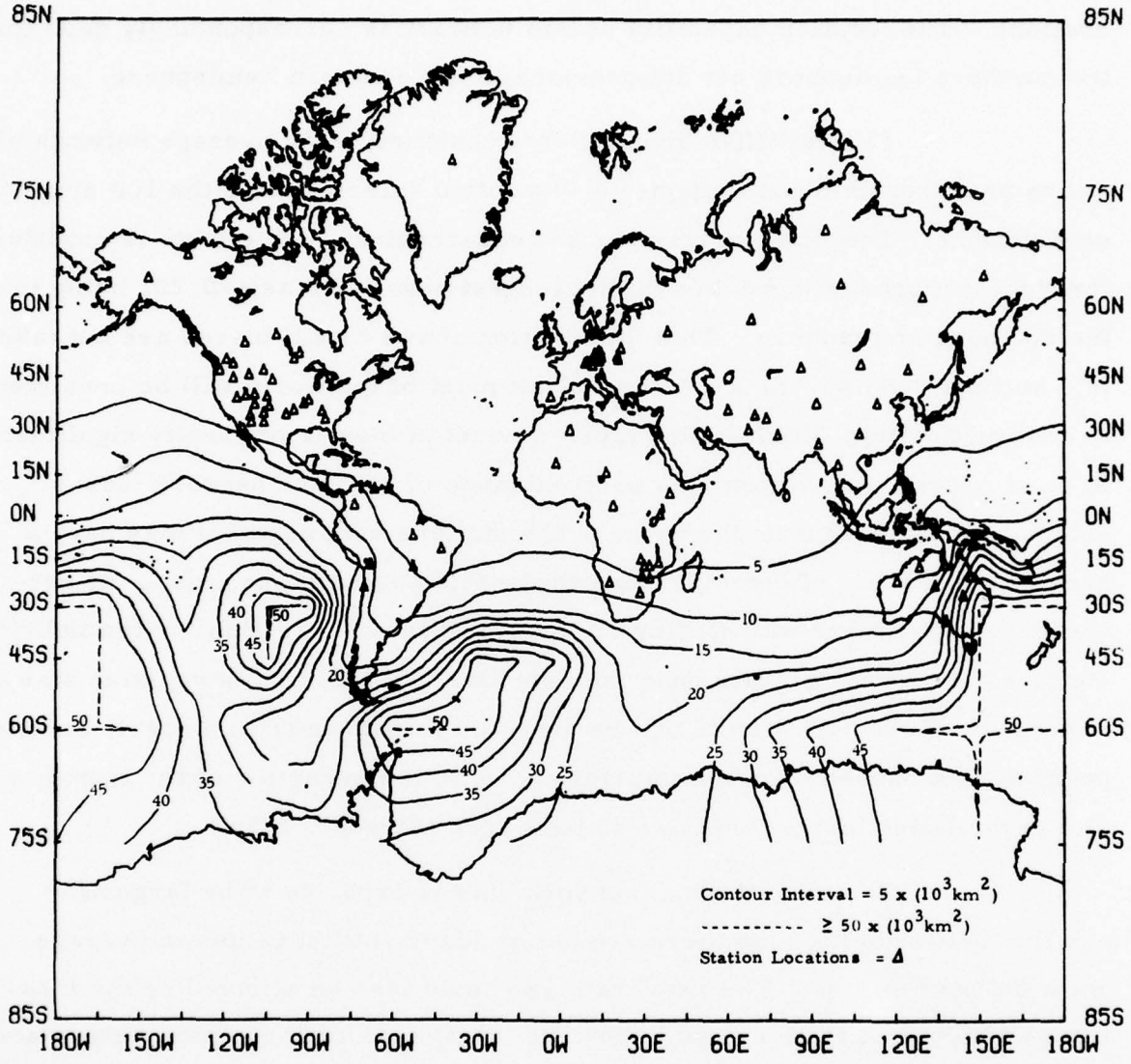

FIGURE VIII-5

95% ERROR ELLIPSE AREAS FOR 100 STATION NETWORK

limit of 50,000 km^2 is placed on the area contours due to contouring considerations. The location capability of this network is correspondingly good for the northern hemisphere but deteriorates in the southern hemisphere.

Figure VIII-6 shows global contours of the average network bias due to near-receiver path effects (0.05 contour intervals) for the 100 single-site stations. The network bias due to near-receiver path effects is negative throughout most of the world with the largest negative bias, -0.20, being in the southern hemisphere. This distribution shows that if biases are not taken into account events of $m_b = 4.0$ throughout most of the world will be consistently underestimated, although the actual amount of bias is not really significant in most cases. In addition, the predominance of negative network biases seems to indicate that on the average the stations with negative bias have a greater probability of detection than those with positive bias, since the network bias values are weighted by the probabilities of detection for the individual stations. For weak signals near the detection threshold, this negative bias due to near-receiver path effects can be expected to compensate, in part, for the positive bias caused by noise interference with the reception of the signal, although the latter bias is expected to be larger (Ringdal, 1975).

The magnitude of network bias is expected to be larger for smaller networks because there are not as many station values to average down the bias effects. The network bias should also be affected by the locations and types of stations and by source location since these parameters affect the probability of detection for an event.

Figure VIII-7 presents the global contours (contour interval = 1) of the Fisher transformation, $\log_{10}(P_D/(1-P_D))$, of the probability of location by the single-site network of a 4.0 m_b event within an error ellipse of 10,000 km^2. This fixed area is reasonably small and provides an additional indication of the location capability of the network. Comparison of this figure with Figure VIII-5 shows that the shape of the contours in both illustrations are

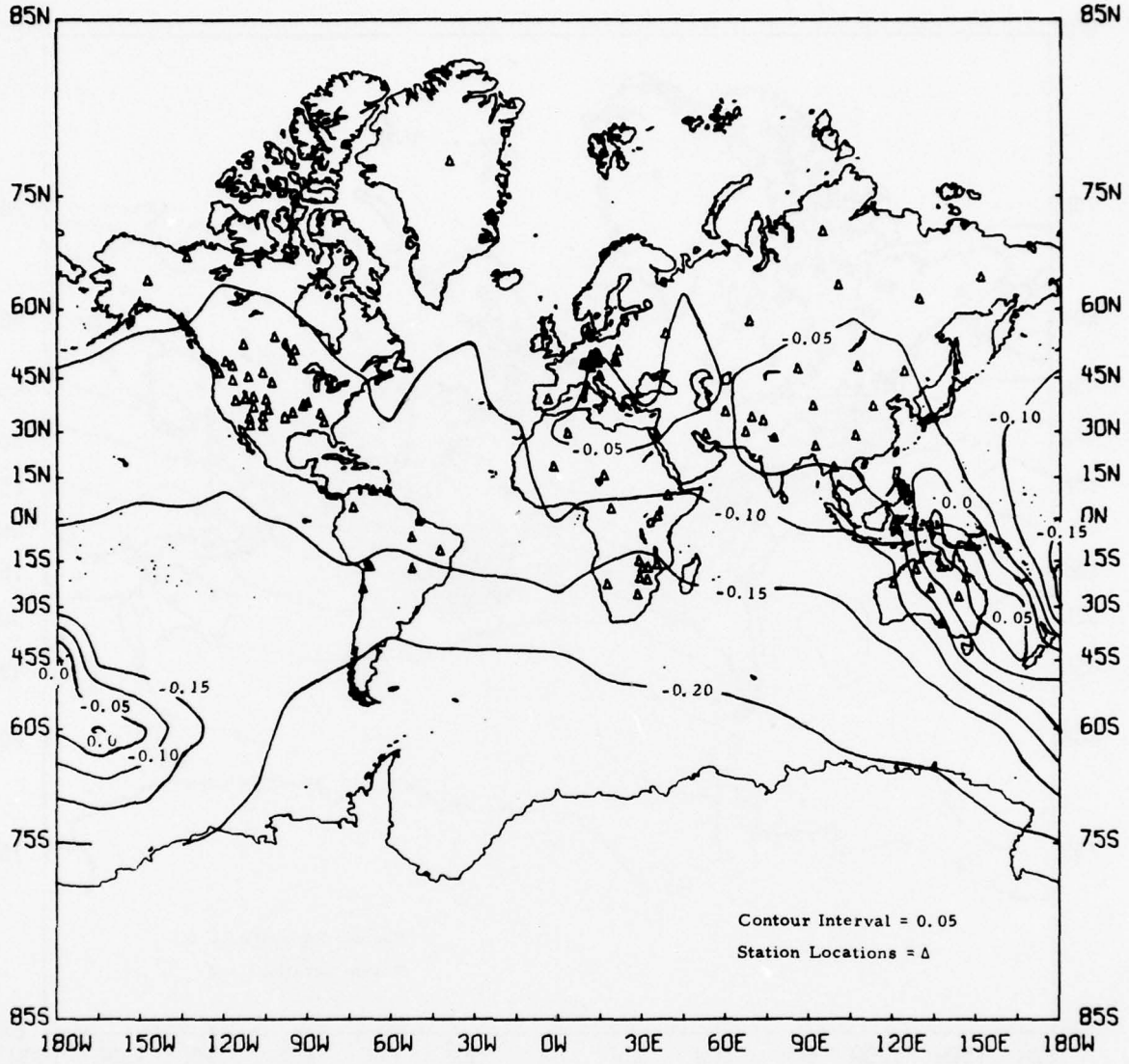

FIGURE VIII-6

AVERAGE NETWORK BIAS FOR 100 STATION NETWORK
(m_b = 4.0)

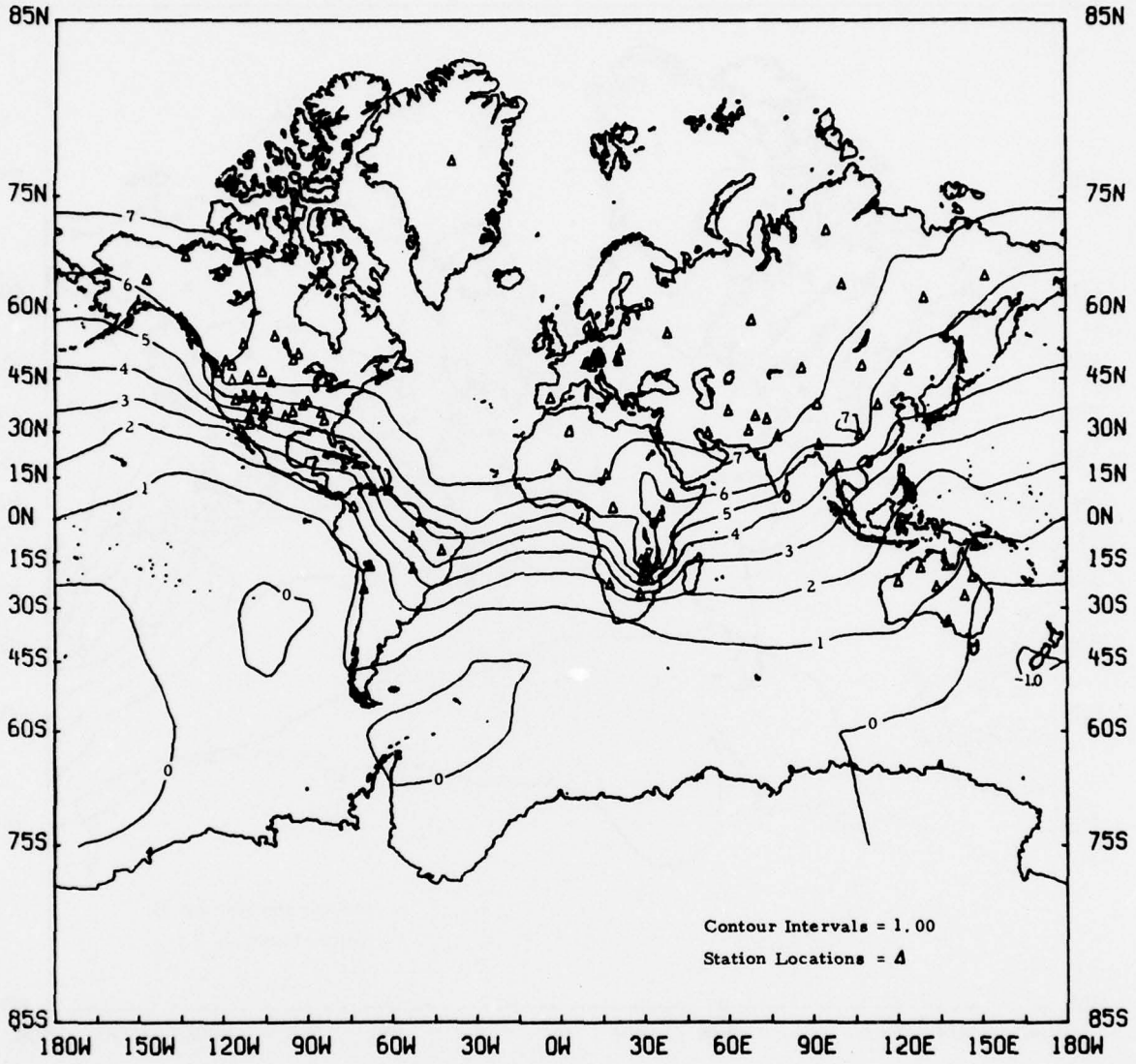

FIGURE VIII-7

LOG ($P_D/(1-P_D)$) OF LOCATION PROBABILITY FOR ARRAY-MODIFIED NETWORK LOCATING AN EPICENTER WITHIN A 10,000 km^2 ERROR ELLIPSE (m_b = 4.0)

similar, as would be expected. The areas of good location capability and poor location capability are the same in both figures.

Figure VIII-8 shows the global contours (contour interval = 1) of the Fisher transformation of network detection probabilities for the network consisting of 28 arrays and 72 single-site stations. As expected, substitution of the arrays for some of the single-site stations improves the detection capability of the network. The 0 contour (50% probability of detection) covers more of the world than is the case when using the other network. The areas of poor detection are more limited and the probabilities of detection are greater.

Figure VIII-9 shows global contours of the 95% error ellipse areas (5,000 km^2 contour intervals) for the network containing the simulated arrays, and has the same contour limitations as Figure VIII-5. This figure illustrates the greater location capability of the array-modified network.

Figure VIII-10 presents global contours of the average network bias (0.05 contour intervals) for the array-modified network detecting the 4.0 m_b event. The greatest negative bias is again in the southern hemisphere, although it is only -0.10 as compared to the previous value of -0.20. In general, the amount of bias is decreased by inclusion of the arrays. This effect is probably due to greater weighting of the array magnitude biases over the single-site biases due to their higher probabilities of detection.

Figure VIII-11 shows the global contours (contour interval = 1) of the Fisher transformation of the probability of location of an event within a 10,000 km^2 error ellipse. This figure also illustrates the greater location capability of the modified network.

Figure VIII-12 shows the contours of the Fisher transformation of the network probability of detection for an event of $m_b = 3.75$ for the network made up of 28 arrays and 72 single-site stations. This magnitude is the

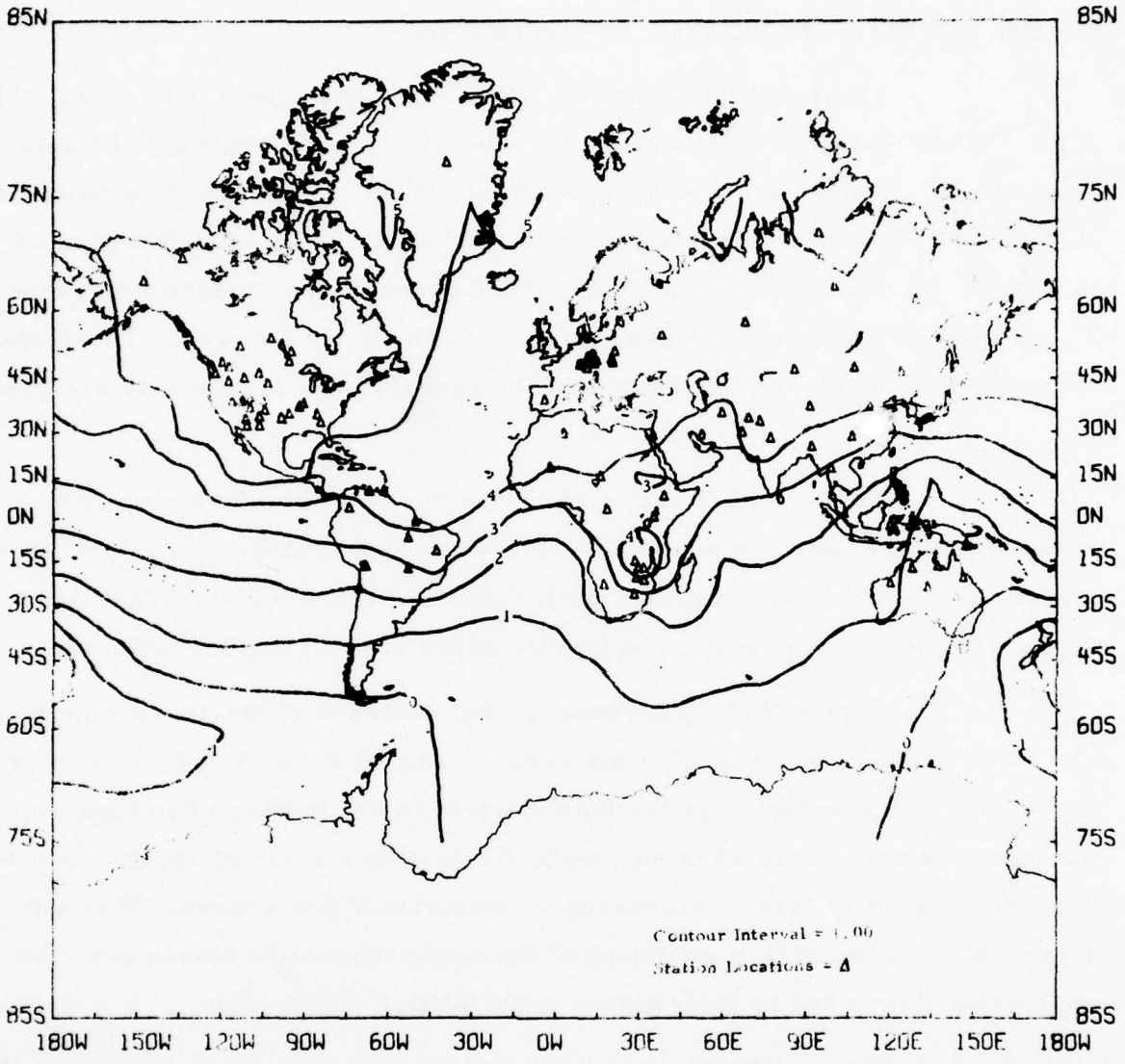

FIGURE VIII-8

LOG ($P_D/(1-P_D)$) OF DETECTION PROBABILITY FOR
ARRAY-MODIFIED NETWORK
(m_b = 4.0)

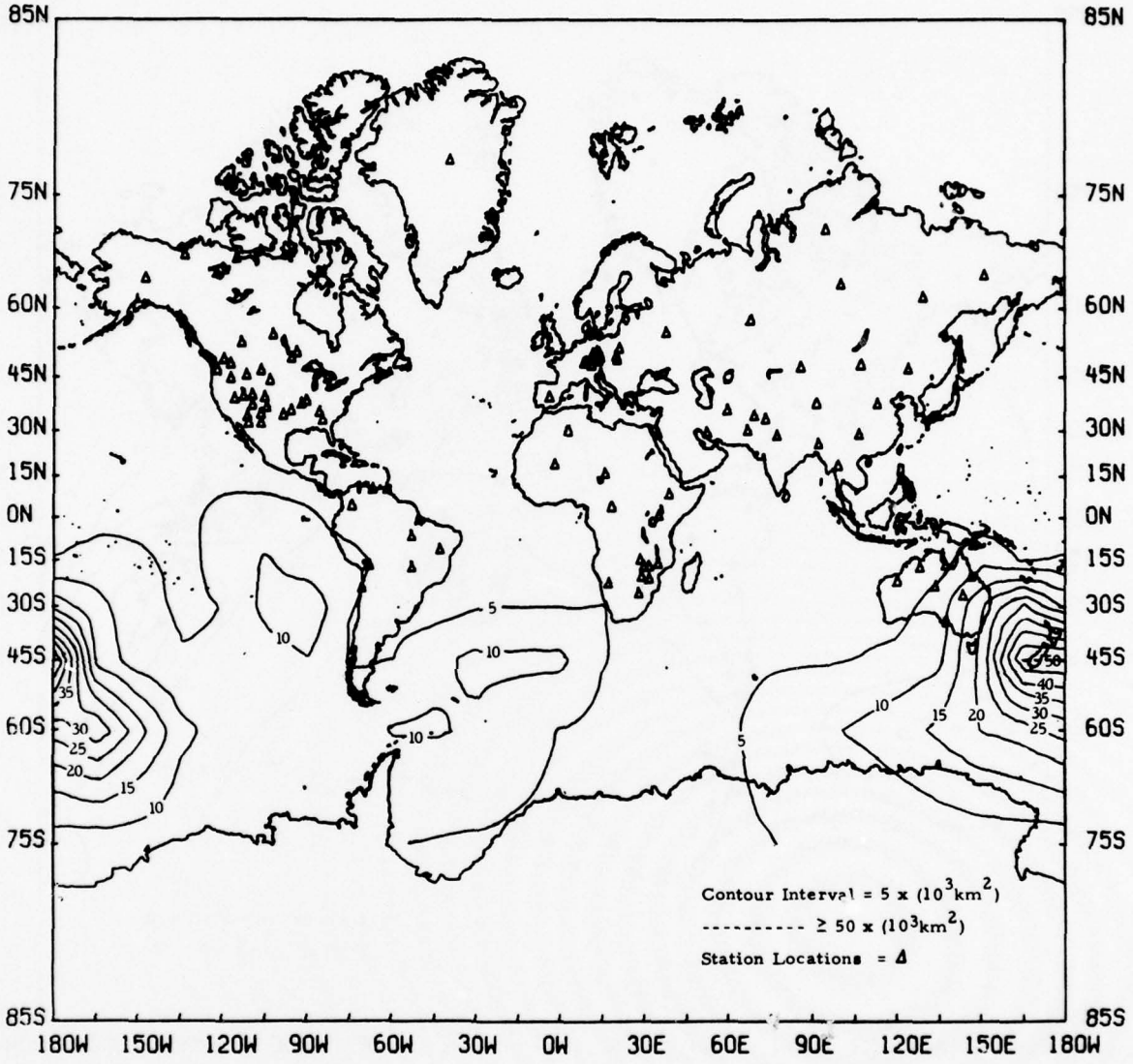

FIGURE VIII-9

95% ERROR ELLIPSE AREAS FOR ARRAY-MODIFIED NETWORK
(m_b = 4.0)

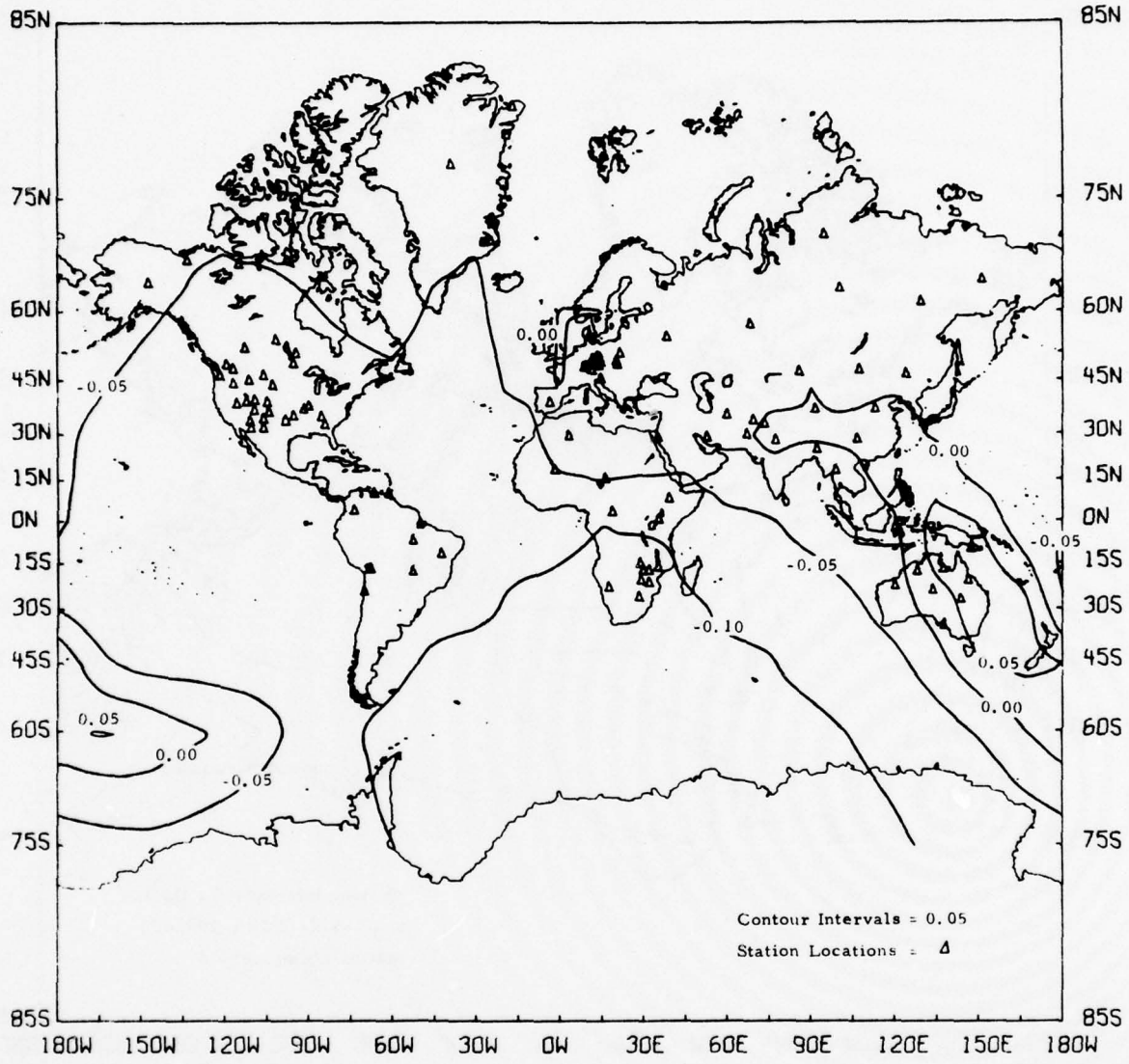

FIGURE VIII-10

AVERAGE NETWORK BIAS FOR ARRAY-MODIFIED NETWORK
(m_b = 4.0)

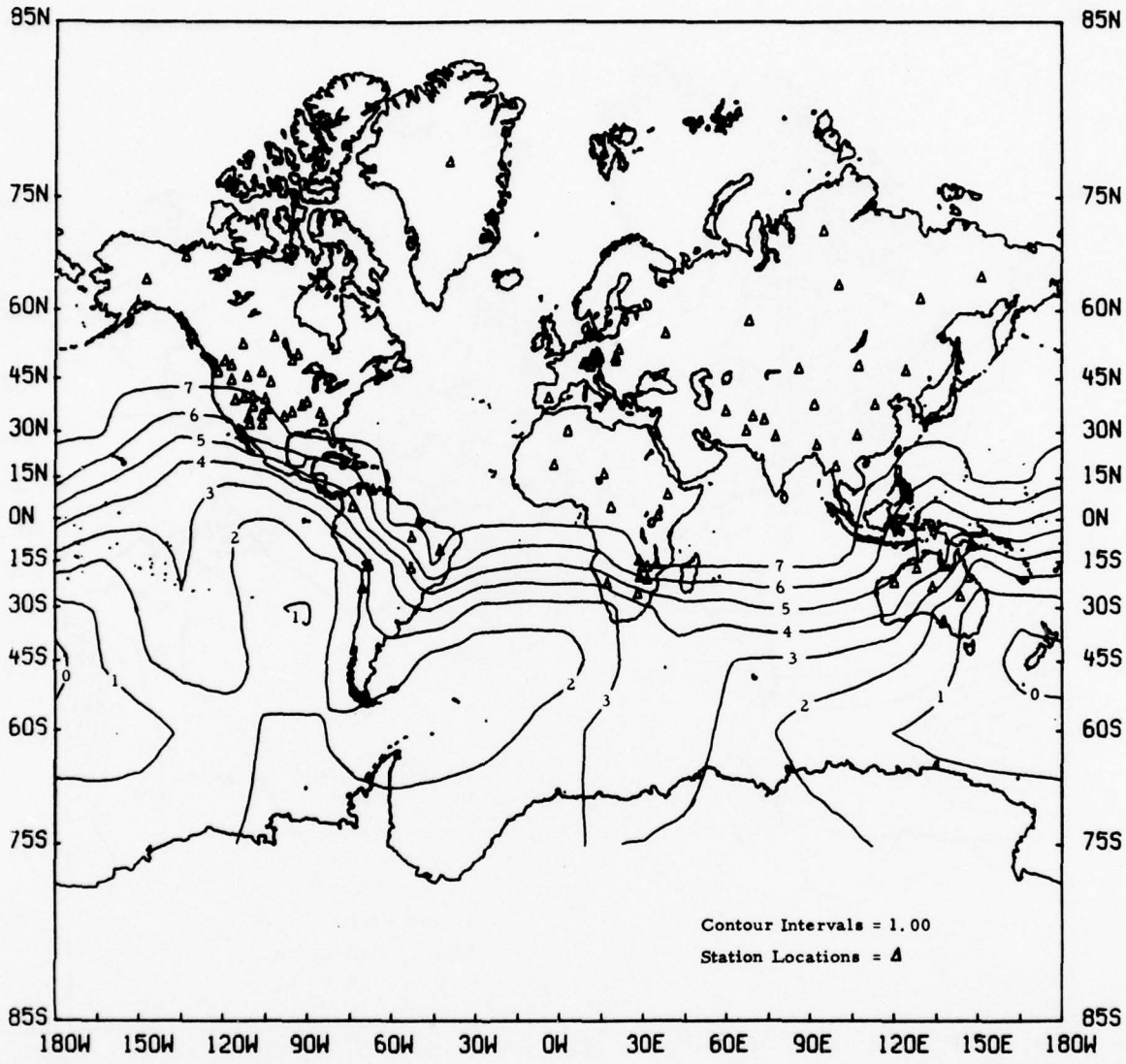

FIGURE VIII-11

LOG ($P_D/(1-P_D)$) OF LOCATION PROBABILITY FOR ARRAY-MODIFIED NETWORK LOCATING AN EPICENTER WITHIN A 10,000 km^2 ERROR ELLIPSE (m_b = 4.0)

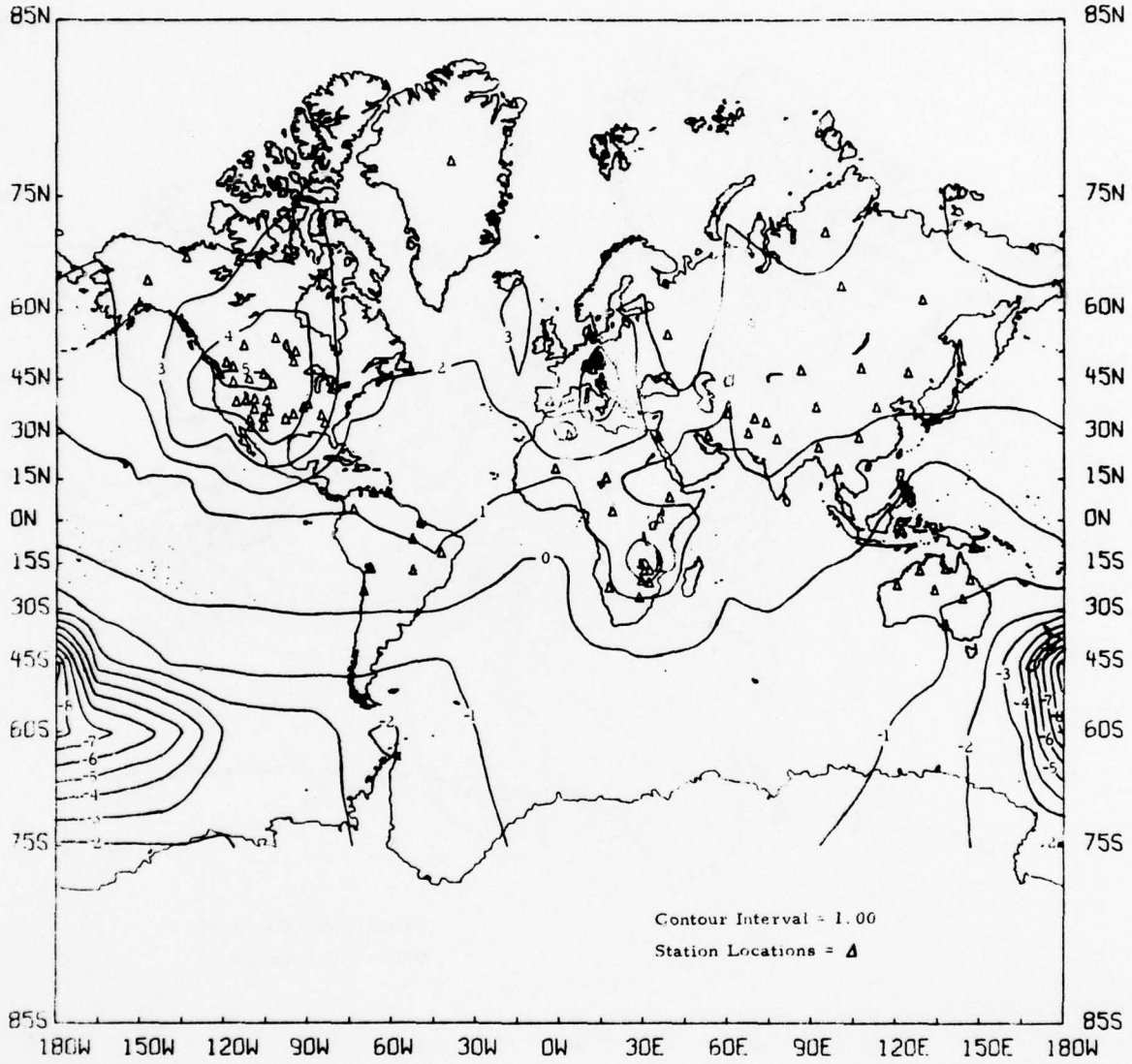

FIGURE VIII-12

LOG ($P_D/(1-P_D)$) OF DETECTION PROBABILITY FOR ARRAY-MODIFIED NETWORK (m_b = 3.75)

approximate lower m_b limit for reasonable detection in the northern hemisphere and was determined by trial-and-error. As can be seen in the figure, the majority of the northern hemisphere still has a probability of detection greater than 50% (0 contour). In fact, the geographic position of the 0 contour is comparable to that obtained with a network of 100 single-site stations detecting an event of $m_b = 4.0$. Although the contour values are generally lower for the array-modified network, the actual difference in values at the high and low extremes is very small as can be seen in Table VIII-3. This observation indicates that a gain in detection capability of nearly 0.25 m_b is obtained by the substitution of 28 arrays for single-site stations.

Figure VIII-13 shows the contours of the 95% error ellipse areas for the 3.75 m_b event and the array-modified network. As expected the location capability is not as great as for the same network with a 4.0 m_b event; however, the location capability is actually better than that observed for the 100 single-site stations location a 4.0 m_b event.

Finally, Figure VIII-14 illustrates the contours of the corresponding average network magnitude bias for the 3.75 m_b event detected by an array-modified network. In general, the negative bias is greater than that observed for the array-modified network detecting a 4.0 m_b event. However, the negative bias for the single-site network detecting a 4.0 m_b event is still greater than either of the above cases.

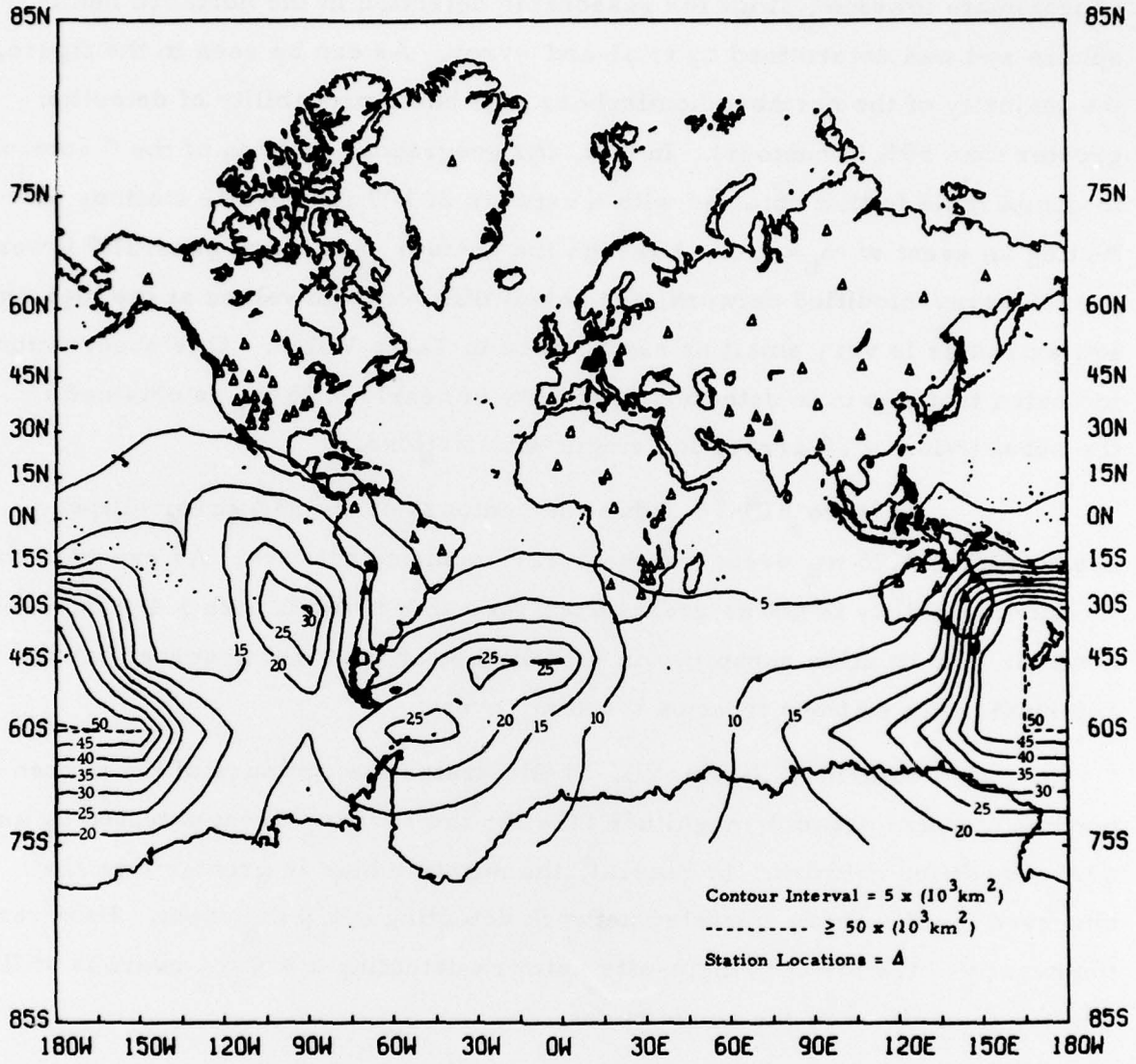

FIGURE VIII-13

95% ERROR ELLIPSE AREAS FOR ARRAY-MODIFIED NETWORK
(m_b = 3.75)

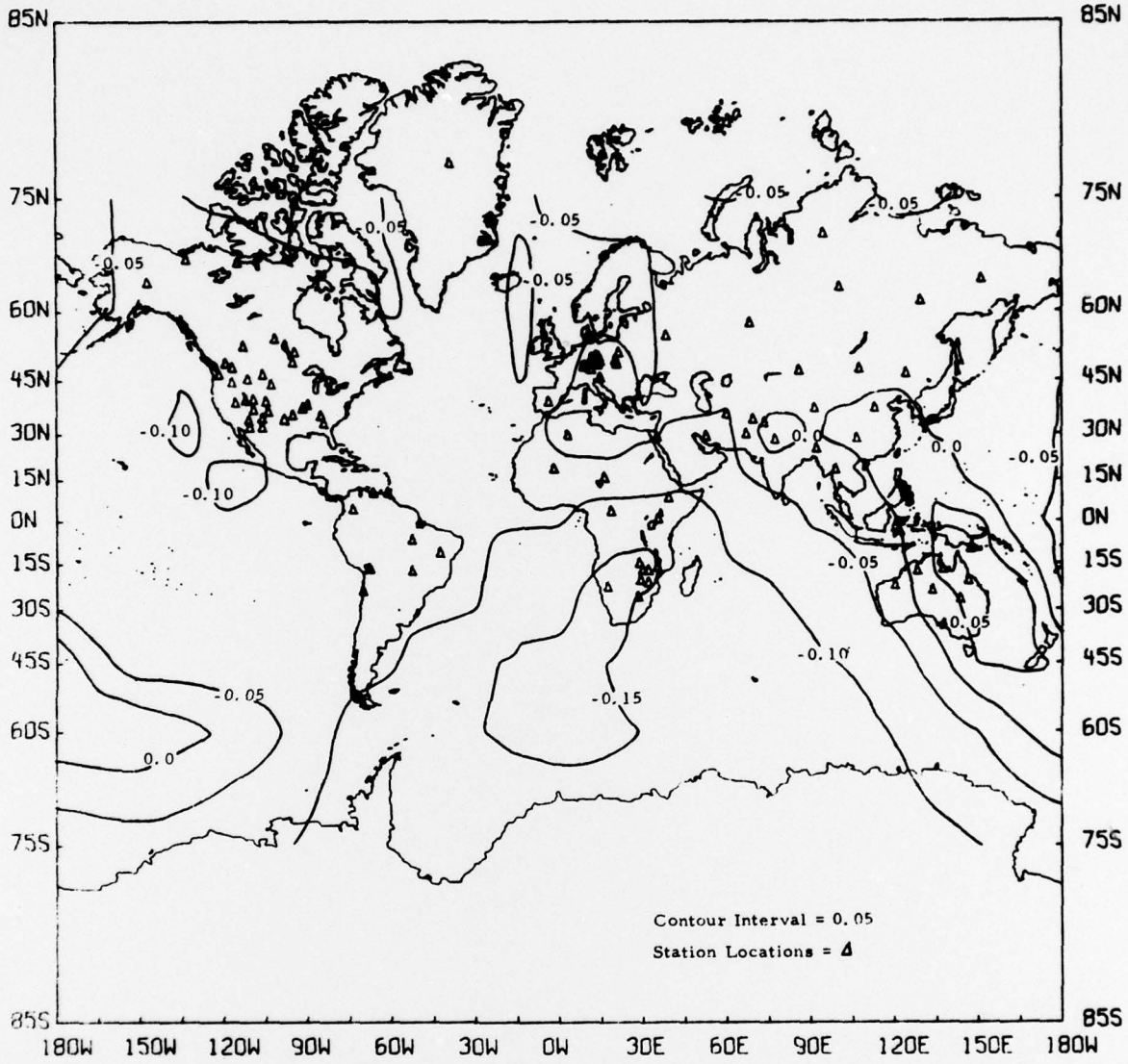

FIGURE VIII-14

AVERAGE NETWORK BIAS FOR ARRAY-MODIFIED NETWORK
(m_b = 3.75)

SECTION IX
CONCLUSIONS

This study indicates that a relationship exists between the magnitude bias, noise, and tectonic structure of a seismograph station. North (1977) has shown that the tectonics of a region appears to be the strongest influence on the magnitude bias observed at seismic stations in that region. This study has also indicated that seismic noise magnitude levels fall into several distinct groups and have an approximately normal distribution within these groups. Given seismic station noise levels and magnitude biases, there is little ambiguity in determining which noise group the seismic station is associated with. Within each group the noise magnitude appears to have an approximately linear relationship with the magnitude bias with the slope being one. Therefore, identification of the geographical distribution of noise groups could be a prime factor in determining the optimum locations for seismic stations.

Although the above relationships suggested by the data appear to be statistically significant empirical observations, more accurate joint measurements of seismic noise and magnitude bias are needed to determine unique relationships between these factors.

The bias and noise appear to be affected by the upper mantle structure, which is related to tectonic structure, in the receiver region. It is suggested that the noise is also dependent on the crustal structure of the receiver region.

A noise study by Sax (1965) showing the relationship of noise to sedimentary structure, the possible enhancement of noise by thick wedges of

recent sediment associated with transgressive shorelines, and the probable association of low noise with the upper mantle velocity inversion in the western United States give some evidence for the relationship between noise and the structure of the crust and upper mantle. It is suggested that bias is affected in a major way by attenuation within upper mantle velocity inversions; whereas site variations of high frequency seismic noise are affected strongly by the depth distribution of seismic energy in trapped surface wave modes. Based on such a seismic noise model, seismic noise levels should be strongly influenced by both crustal and upper mantle structure at the seismic station.

While tectonic structure is clearly related to magnitude bias, it does not seem to be as well correlated with the noise level grouping, at least for the line model. On a world-wide basis, each noise group is observed to include two or three tectonic types. A noise group zone may also map geographically across two or more tectonic provinces. Within a tectonic province, several different noise group zones may be encountered. The models developed in this study make it possible to develop a scheme for assigning bias and/or noise values to locations throughout the world. In estimating the bias and noise values at a site, knowledge of the noise group is the most desirable factor although it is not necessary.

Areas of the world exist where the short-period noise is fairly stable all year-round. The boundaries of these areas follow the coastlines for the most part, but there are regions where they cut across the continental boundaries. The exact reason for this behavior is not known, but may, at least in part, be correlated with transgressive shorelines and the associated coastal or continental shelf accumulations of recent soft sedimentary layers.

By using the bias-noise-tectonics relationship to assign station parameters and by limiting the sites to regions inside the zones of relatively stable noise, the detection capability of a hypothetical network of 100 single-sensor stations relatively insensitive to seasonal changes was evaluated. The

probability of detection of an 4.0 m_b event for this network is greater than 50% for the most of the Earth's continental area. The detection capability can be strengthened by replacing some of the single sensors by arrays. In this study, it has been found that substitution of 28 arrays for single sensors in the lower latitudes and around the Pacific Ocean results in a 0.25 m_b gain in detection capability.

In order to obtain a more definite idea of the relationship between magnitude bias, noise, and tectonic structure, a much larger data base of better data is needed. Some bias might exist due to the large numbers of U.S. stations used in this study. Combining platform and fold belt regions into one tectonic type might not be valid if more data were available. However, due to the small amount of data available for this study, it was necessary to limit the number of classes in order to make the statistics more realistic. In addition, other methods for removing the effects of ocean noise could be investigated to determine what effect thay may have on the relationship. Since the noise present at a given site is not entirely due to propagating ocean noise, it might also be possible to study additional corrections for changes in the crustal and upper mantle earth structure and for local geology, if these factors are known.

Since, as mentioned earlier, bias and noise are primarily dependent on upper mantle structure and noise is also strongly dependent on crustal structure, representative models of crustal and upper mantle structure might be used to further study the bias and noise at the surface. Investigation of bias would involve looking at the attenuation and absorption of P-waves in the upper mantle and crust and noise investigations would involve looking at the different Rayleigh wave modes as a function of depth in the crust and upper mantle. Correlation of noise zoning with these and other geological and geophysical parameters would allow better definition of the boundaries of the noise zones. This would also strengthen the use of the noise zones in siting and evaluating stations.

SECTION X
REFERENCES

Blandford, R. R., and E. I. Sweetser, 1978; Short-Period Earthquake Coda Shape as a Function of Geology and System Response, Teledyne Geotech, Alexandria, VA.

Binder, F. H., Burg, J. P., 1966, Array Research-Wavenumber Analysis of TFO Long-Noise Sample, Special Report No. 17. Texas Instruments Incorporated, Contract Number AF 33(657)-12747.

Bradner, H., L. G. de Jerphanion, and R. Langlois, 1970; Ocean Microseism Measurements with a Neutral Buoyancy Free-Floating Midwater Seismometer, BSSA, Vol. 60, No. 4.

Burg, J. P. ane G. C. Burrell, 1967; Array Research-Analysis of K-line Wavenumber Spectra from the TFO Long Noise Sample, Special Report No. 23, Texas Instruments Incorporated, Contract Number AF 33 (657)-12747.

Capon, J., 1969; Investigation of Long-Period Noise at the Large Aperture Seismic Array, Journal of Geophysical Research, Vol. 74, No. 12.

Clawson, G. E., and K. F. Veith, 1972; Magnitude from Short-Period P-Wave Data, BSSA, 62, No. 2.

Dinger, J. E., 1963; Comparison of Ocean-Wave and Microseism Spectrums as Recorded at Barbados, West Indies, Journal of Geophysical Research, Vol. 68, No. 11.

Douze, E. I., 1967; Short-Period Seismic Noise, BSSA, Vol. 57, No. 1.

Evernden, J. F., and D. Clark, 1970b; Study of Teleseismic P...II Amplitude Data, Phys. Earth Planet. Interiors, 4, 1-31.

Evernden, J. F., and J. Filson, 1971; Regional Dependence of Surface-Wave versus Bodywave Magnitudes, Journal of Geophysical Research, 76, No. 14.

Evernden, J. F., and W. M. Kohler, 1976; Bias in Estimates of m_b at Small Magnitudes, Bulletin Seismological Society of America, 66, 1887-1904.

Fix, J. E., J. G. Swanson, and W. D. Ballard, 1973; Study of Selected World-Wide Seismograph Network Stations, Seismic Array Analysis Center Report No. 11, Teledyne Geotech, Garland, TX.

Geotechnical Corporation, The, 1965; Seismic Noise Survey, Long-Range Seismic Measurements Program, Volume 2, Technical Report No. 65-25, Garland, TX.

Griffin, J. N., 1963; Final Report, Field Study of Variation in Characteristics of Seismic Noise and Signals with Geological and Geographic Environment, Volume 1, United Electrodynamics Incorporated, Report Number VT/078-29, Alexandria, VA.

Hair, G. D., J. H. Funk, and Research Staff, 1964; Noise Study, Special Report No. X, Texas Instruments Incorporated, Dallas, TX.

Hasselmann, K., 1963; A Statistical Analysis of the Generation of Microseisms, Reviews of Geophysics, Volume 1, No. 2.

Haubrich, R. A., and K. McCamy, 1969; Microseisms-Coastal and Pelagic Sources, Rev. Geophysics, Volume 7, No. 3.

Herrin, E., 1968; Seismological Tables for P Phases, BSSA, 58, No. 4.

Johnson, W. A., J. A. Bonner, J. P. Bury, and G. D. Hair, 1968; Network Studies-Noise Analysis Advanced Array Research, Special Report No. 6, Texas Instruments Incorporated, Contract Number F33657-78-C-0708-P001.

Kummel, B., 1970; History of the Earth, An Introduction to Historical Geology, W. H. Freeman and Company, San Francisco, CA, 87-112.

Longuet-Higgins, N. S., 1950; A Theory of the Origin of Microseisms, Phil.-Trans. Ray. Loc. London, Sep. A, No. 243.

National Earthquake Information Center, 1970; Seismograph Station Abbreviations, U. S. Department of Commerce, Environmental Science Services Administration, Coast and Geodetic Survey, Rockville, MD.

North, R. G., 1977; Station Magnitude Bias - Its Determination, Causes, and Effects, MIT Lincoln Laboratories Technical Note 1977-24.

Ostle, B., 1963; Statistics in Research, The Iowa State University Press, Ames, IA, 119,123, 528-543.

Pena, C., 1967; Seismic Noise Survey, Volume 3, Long-Range Seismic Measurment Program, Technical Report No. 67-19, Teledyne Geotech, Garland, TX.

Ringdal, F., 1975; Maximum Likelihood Estimation of Seismic Event Magnitude from Network Data, Technical Report No. 1, Texas Instruments Report No. ALEX(01)-TR-75-01, AFTAC Contract Number F08606-75-C-0029. Texas Instruments Incorporated, Dallas, TX.

Sax, R. L., 1965; Seismic Noise Models, Proceedings of the IEEE, 53, 1870-1872.

Sax, R. L., 1970, Estimation of P-Waves Using Vertical and Small Aperture Horizontal Arrays, Seismic Data Laboratory Report No. 257, Teledyne Geotech, Contract Number F33657-70-C-0941.

Smith, P. J., 1973; Topics in Geophysics, MIT Press, Cambridge, MA, 131.

Snell, N. S., 1976; Network Capability Estimation, Technical Report No. 4, Texas Instruments Report No. ALEX(01)-TR-76-04, AFTAC Contract

Number F08606-76-C-0011, Texas Instruments Incorporated, Dallas, TX.

Strauss, A. C. , 1976; Preliminary Evaluation of the Seismic Research Observatories, Technical Report No. 2, Texas Instruments Report No. ALEX(01)-TR-76-02, AFTAC Contract Number F08606-76-C-0011, Texas Instruments Incorporated, Dallas, TX.

Swindell, W. H., and N. S. Snell, 1977; Station Processor Automatic Signal Detection System, Phase I: Final Report, Texas Instruments Report No. ALEX(01)-FR-77-01, AFTAC Contract Number F08606-76-C-0025, Texas Instruments Incorporated, Dallas, TX.

Toksöz, M. N., and R. T. Lacoss, 1968; Microseisms: Mode Structure and Sources, Science, Volume 159, P. 872.

Unger, R., 1977; Automatic Detection, Timing and Preliminary Discrimination of Seismic Signals with the Instantaneous Amplitude, Phase, and Frequency, Technical Report No. 4, Texas Instruments Report No. ALEX(01)-TR-77-04, AFTAC Contract Number F08606-77-C-0004, Texas Instruments Incorporated, Dallas, TX.

Wirth, M. H., 1970; Estimation of Network Detection and Location Capability, Seismic Data Laboratory Research Memorandum, Teledyne, Geotech, Alexandria, VA.